Research Square

Preprints are preliminary reports that have not undergone peer review.
They should not be considered conclusive, used to inform clinical practice,
or referenced by the media as validated information.

A New Microfluidic Concept for Successful in Vitro Culture of Mouse Embryos

Vanessa Mancini
University of Leeds
Paul McKeegan
University of Hull
Alexandra C. Schrimpe-Rutledge
Vanderbilt University
Simona Gabriela Codreanu
Vanderbilt University
Stacy D. Sherrod
Vanderbilt University
John A. McLean
Vanderbilt University
Helen M. Picton
University of Leeds
Virginia Pensabene (V.Pensabene@leeds.ac.uk)
University of Leeds

Research Article

Keywords: assisted reproductive technologies, IVF, embryo culture, microfluidics, mice

Posted Date: February 17th, 2021

DOI: https://doi.org/10.21203/rs.3.rs-201942/v1

License: This work is licensed under a Creative Commons Attribution 4.0 International License.
Read Full License

A new microfluidic concept for successful *in vitro* culture of mouse embryos

V. Mancini[1] and P.J McKeegan[2,5], A.C. Rutledge[3], S.G. Codreanu[3], S.D. Sherrod[3], J.A. McLean[3], H.M Picton[2], V. Pensabene[1,4*]

[1]School of Electronic and Electrical Engineering, University of Leeds, Leeds, UK, LS2 9JT.

[2] Reproduction and Early Development Research Group, Discovery and Translational Science Department, Leeds Institute of Cardiovascular and Metabolic Medicine, School of Medicine, University of Leeds, UK, LS2 9JT.

[3] Center for Innovative Technology (CIT), Department of Chemistry, Vanderbilt University, 7300 Stevenson Center Lane, Nashville, TN 37235.

[4] Leeds Institute of Medical Research, University of Leeds, UK, LS2 9JT.

[5] Centre for Anatomical and Human Sciences, Hull York Medical School, University of Hull, Hull, UK, HU6 7RX

Keywords: assisted reproductive technologies, IVF, embryo culture, microfluidics, mice

ABSTRACT

Innovative techniques for gene editing have enabled accurate animal models of human diseases to be established. In order for these methods to be successfully adopted in the scientific community, the optimization of procedures used for breeding genetically altered mice is required. Among these, the *in vitro* fertilization (IVF) procedure is still suboptimal and the culture methods do not guarantee the development of competent embryos. Critical aspects in traditional *in vitro* embryo culture protocols include the use of mineral oil and the stress induced by repetitive handling of the embryos.

A novel microfluidic system was designed and fabricated in poly dimethyl siloxane (PDMS) to allow for efficient *in vitro* production of mouse embryos. Culture experiments conducted by completing the industry gold standard Mouse Embryo Assay excluded any harmful fluidic stress and plastic toxicity. The developmental competence of the embryos developed in the device was consistently confirmed by high blastocyst rate (>80%), hatching and outgrowth rate, and matched with analysis of energy substrate metabolism and expression of genes related to implantation potential.

Metabolomics analyses of spent culture media allowed for biologically important metabolite changes to be observed throughout embryo development, and for identification of specific overrepresented metabolic pathways affected by the microfluidic environment. Moreover, mass spectrometry data identified plastic-related compounds released in medium, and confirmed leaching of low molecular weight species into the culture medium that might be associated to un-crosslinked PDMS.

Finally, these data show the potential for the system to study preimplantation embryo development and to improve the embryo culture techniques used for human assisted conception.

Introduction

Genetically altered (GA) mice are used extensively to study the function and regulation of genes and their role in human development, as well as human health and disease. Historically mouse models have been widely used to advance research into ageing [2], [3] breast cancer [4], [5], metabolic disorders, diabetes, obesity as well as rare diseases for drug discovery [6], [7]. Almost 50% of the total amount of animals used for scientific research are genetically modified animals, the majority of which are mice [1]. In recent years a resurgence in the use

of GA mouse models for medical research and pharmaceutical industry has occurred thanks to the introduction of sequencing methods, and our ability to combine genetic engineering technologies such as CRISPR/Cas9, with methods used for microinjection, nuclear transfer as well as *in vitro* fertilisation (IVF), embryo and stem cell culture and derivation. These research tools are invaluable for the production of “humanised” mice, in which a particular mouse gene is replaced by its human counterpart known to be associated with a specific human disease. The animal facilities for breeding GA mice are increasingly reliant on assisted reproduction technologies (ART) to generate embryos *in vivo* and *in vitro* for manipulation and cryopreservation to build research banks of GA embryos or to distribute GA embryos or animals to the research community [9], [10]. High standards of animal welfare are required to support the processes involved in the generation of GA animals for research in order to generate, robust, high-quality data [8]. Many mouse GA facilities therefore need to implement significant changes in their breeding protocols and production methods in order to maximise efficiency, reduce animal suffering, improve throughput and increase pregnancy and birth rates of genetically modified animals [11]–[13].

The *in vitro* production of mouse embryos typically involves the culture of multiple embryos in 5-100µl microdrops of specialised embryo culture medium [14] in Petri dishes covered with a layer of mineral oil to prevent media evaporation and associated changes in pH and osmolarity (Fig. 1.a). Single cell, fertilised zygotes or early cleavage staged preimplantation embryos derived *in vivo* or *in vitro* are transferred to sterile microdrops of pre-equilibrated, defined culture media and allowed to develop undisturbed in a humidified and gassed incubator environment for 2-5 days until they reach the blastocyst stage of development. When ready for transfer, mouse blastocysts are aspirated and injected in the oviduct or uterus by traditional Surgical Embryo Transfer (SET) techniques or by Non-Surgical Embryo Transfer (NSET) [12]. Embryo handling for both SET and NSET transfers occurs by manual pipetting, which is labour intensive, time consuming, not repeatable and complicated by the presence of the mineral oil over layer in the culture dish. First implemented in 2009, NSET techniques are now adopted globally and are of similar or improved efficiency to SET [11], [12], [15]. However, it is widely recognised that not all embryos grown *in vitro* have the same potential to develop to the blastocyst stage or to implant and produce a pregnancy following transfer. Indeed, considerable research effort in a range of species has confirmed that embryo development and implantation efficiency are highly variable and are critically dependent on a range of factors that include: the embryo development stage at transfer [16] and the creation and use of species specific, optimal culture environments [17]. Higher implantation and pregnancy rates post transfer have been reported when culturing embryos to the morula or blastocyst stage *in vitro* prior to transfer, a procedure requiring up to 4 days of culture in the mouse and 5-8 days in other mammalian species [18]–[20].

Since the 1990’s, microfluidics has been proposed as a new approach to optimise the specialized *in vitro* requirements for successful ART. In 2002, Hickman utilized a microfluidic device to evaluate the effect of dynamic medium environment through the different stages of embryo development [21]. Later in 2006 and 2010 Cabrera and Heo observed that dynamic perfusion was essential for successful development of 1-cell mouse zygotes in a funnel-shaped microfluidic device, positively influencing hatching rate and cell number [22], [23]. While implantation rates and numbers of ongoing pregnancies were similarly improved by the dynamic culture, the new approach was comparable to the traditional microdrop culture approach. More recently, Swain summarized the benefits and limitations of the microfluidic approach for clinical procedures in ART (these include: oocyte maturation, manipulation, embryo culture, cryopreservation and non-invasive quality assessment) [24]. LeGac also presented a comprehensive assessment of the beneficial effect of volume reduction on single and group embryo culture using a microfluidic chamber that supported improved blastocyst development without altering birth rate [25]. While the interest in the use of these microfluidic

systems is still high, extensive scientific analyses to assess safety, consistency and accuracy remain and the long-term impact of culturing embryos in microfluidic devices is not completely understood.

Material toxicity is one of the main concerns, mostly due to the fact that the majority of the research prototype devices used are fabricated “in-house” using manufacturing processes that are difficult to control. The use of polymers that are not medical graded, impure or not completely polymerized affects the safety of the materials in ART. Plastics and chemical residues present in manufacturing consumable plastics will not only affect the viability of the embryos, but may also trigger long-term adverse effects on subsequent foetal development [26]–[30].

Most of the microfluidic devices proposed in literature for mouse embryo culture are manufactured in poly dimethyl siloxane (PDMS). Data relative to blastocyst rate and birth rate obtained with different devices support the safety of this material. Alternative materials, such as poly methyl methacrylate, polycarbonate, cyclic olefin polymers and copolymers and the most common polystyrene are common thermoplastic materials used in industrial manufacturing of disposable plastic. Most of these are used for microfluidic manufacturing with cheap and fast processes but published evidence does not exclude their long term toxicity [31]. In 2004, Wheeler [32] compared the development of embryos cultured in a microfluidic channel under static conditions, manufactured in silicon/borosilicate and PDMS/borosilicate. In this study, both devices resulted in improvement of embryo cleavage and blastocysts rates compared to the microdrop culture method. However, the results were not consistent with the Mouse Embryo Assay (MEA), which is the industry gold standard for quality control of all lab-ware, media and any other tools that come in contact with the embryos during the ART process [33].

Interestingly, the main advantage of the microfluidic approach is the reduction of the culture media volumes used relative to the standard microdrop culture methods. Over the last two decades, there has been a move in human ART towards embryo culture in ultra-microdrops (1.5 to 2 µl) of medium [34]. This technique supports acceptable implantation and pregnancy rates, and its efficacy has been attributed to the increased availability of autocrine and paracrine growth factors secreted by embryos grown in reduced drop volumes. These growth promoters would normally be diluted out by the larger volumes used in conventional microdrop culture strategies [35]–[37].

In recent years, the variable developmental competence (quality) of embryos produced using ARTs has led to the development of a range of invasive and non-invasive clinical and research methods that can be used to directly quantify and hence predict embryo implantation and pregnancy potential [39]. These embryo quality assays can now be used to generate an in-depth understanding of the impact of microfluidic culture and the reduced culture volumes on the health and developmental potential of *in vitro*-derived mouse embryos. Morphokinetics (embryo morphology, cleavage rate, timing, cell number and fragmentation) [40]–[44], embryo energy metabolism [44]–[46], blastocyst hatching and outgrowth rates [47], blastocyst production and cell count, and blastocyst cell allocation to the inner cell mass vs. the trophectoderm [48]–[50] as well as in-depth molecular analysis of trophectoderm biopsies represent biomarkers of blastocyst competence that can be evaluated *in vitro* and can be used to optimize the microfluidic technology before moving to *in vivo* testing, thus avoiding unnecessary sacrifice of animals.

While some of these methods have been used for validation of microfluidic prototypes, metabolic, genetic and epigenetic signatures of embryos developed in microfluidic devices have never been compared with those of embryos cultured in traditional microdrops. Preimplantation embryo development is defined by specific patterns in gene expression associated with cell divisions, starting from the fertilized zygote and progressing through embryonic genome activation to the blastocyst stage of development. The sequence takes

approximately 4.5 days in mice. In the last decade, global gene expression analyses have led to the characterisation of the expression patterns of thousands of genes that have specific functions during mouse embryo preimplantation development [51], [52]. Analysis of candidate genes known to be involved in trophoblast differentiation (such as caudal type homeobox *Cdx-2* [53], TEA domain family member 4 *Tead4* [54] and E74-like factor 5 *Elf5* [55]) and ICM/epiblast development (such as octamer-binding transcription factor *Oct-4* [56] and SRY (sex determining region Y)-box 2 *Sox2*), or transcriptional repressors such as the methycytosine binding protein genes Mbd [57], can be used to provide valuable insights into the potential effects of the microfluidic environment on key markers of embryo development and health [58],[59].

In the current study we developed and fabricated a novel, oil-free disposable microfluidic device in PDMS, in which fertilized 1 cell/ two ProNuclei (2PN) stage murine zygotes can be grown to the expanded blastocyst stage *in vitro* and retrieved for subsequent embryo transfer (Fig. 1.B). In order to minimize any fluid dynamic shear stress during embryo handling and their injection into the device, the microfluidic design was optimized using Finite Element Modelling (FEM); the model also verified the efficiency of the embryo loading and nutrient diffusion in the system. The potential toxicity of PDMS was assessed by performing the MEA, in which embryo cleavage, blastocyst development, hatching and outgrowth rate were used as predictive indexes of embryo health and implantation potential. The embryo culture conditions were optimized by studying the effect of group embryo culture on blastocyst development rate, performing metabolic profiling and determining mitochondrial polarization ratios. Furthermore, the gene expression profiles of blastocysts developed inside the system were compared to those cultured in traditional microdrops using real-time PCR analysis (Fig. 1.C). These data were used to exclude potential genetic alterations induced by the different environment and culture methods. Finally, global untargeted metabolomics was used to identify PDMS-released compounds from culture media extracted from the microfluidic device at different time points (24 h and 5 days).

Based on this extensive evaluation, we demonstrated the ability of our microfluidic system to improve methods for culturing mouse preimplantation embryos, and that our microfluidic devices are compatible with generic lab equipment (such as optical microscopes, bench-top incubators) and so are amenable to traditional embryo handling and analytical procedures (e.g. loading and retrieval with micropipettes) that are routinely used in ART as well as with research methods such as fluorescent staining and fixation.

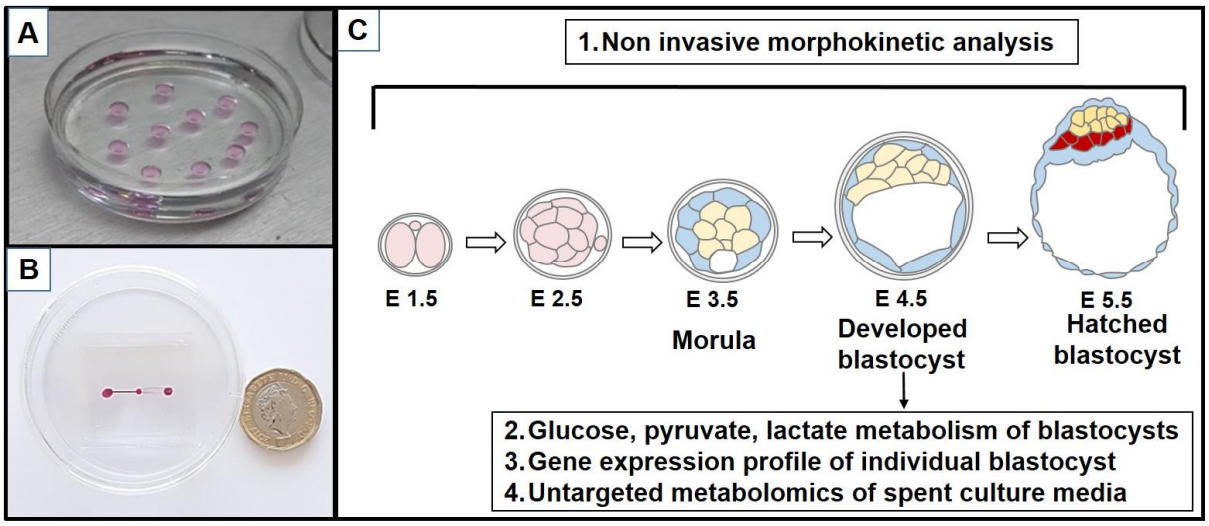

Figure 1 *A) Traditional microdrop culture. B) Image of the fabricated PDMS microfluidic device in a traditional 60 mm petri dish used for embryo culture. Red dye indicates inlet and outlet ports and microfluidic channels. The device is sitting within a standard 60mm culture dish.*

Image shown next to a UK 1 pound coin for scale. C) Schematic of in vitro murine embryo development in the device. Non-invasive analytical methods can be used to monitor, grade and stage the embryos during culture. Endpoint embryo quality analyses (genetic and metabolic profiling) that can be performed for each individual embryo.

Results

Microfluidic design is compatible with standard embryo culture methods. The microfluidic device presents two fluidic ports connected to a culture chamber by two microfluidic channels (Fig. 2). The volume of medium in the chamber is 400 nL, thus significantly reduced compared to the traditional 5-50 µL used in microdrop technique and below the volume limit (1.5-2 µL) used in the ultra microdrop method. The inlet and outlet channels are present at different heights and positioned in 2 different layers (top and bottom): the single inlet channel is 200 µm in height and 250 µm in width. The narrow outlet channels are at lower level and 30 µm tall, thus smaller than the size of a mouse embryo (diameter ~60 µm). These dimensions allow the embryos to be loaded and to reach the chamber, where they cannot flow any further (see Video 1 in Supp. Mat.). Embryos are left undisturbed to grow up to blastocysts (diameter ~100 µm, 3 days) and then aspirated back through the inlet channels to proceed with the transfer. The final device, measuring 4 by 4 cm, can be placed in a standard 60 mm IVF culture dish, sterilized and used in a MINC™ Mini incubator (Figure 1.B).

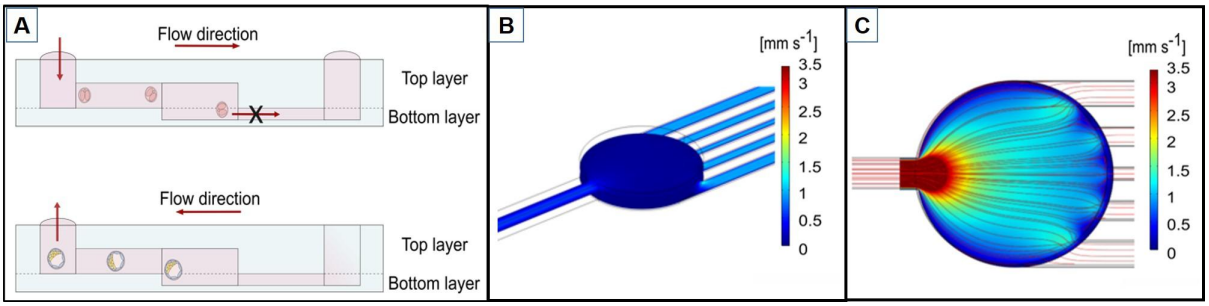

Figure 2. *Microfluidic device design. A) Embryos are introduced from the inlet port, guided by capillarity force in the culture chamber through the inlet channel. Being the embryos diameter bigger than the outlet channels, they remain trapped in the chamber. Once developed embryos are aspirated from the inlet port. B) The Finite Element Model of the average velocity shows an increase in the lateral channels compared to the main chamber owing to their small dimensions. C) Fluid flow analysis of velocity magnitude surface plot shows the velocity field generated in the fluidic systems.*

Minimal stress or damage observed by flow and shear stress during loading and through the development process in the microfluidic device. The design of the device allows for the capture of the embryos in the middle chamber owing to the increased hydraulic resistance encountered when reaching the chamber (Fig. 2). Furthermore, the wall shear stress (*WSS*) generated within the channels during loading and retrieval reaches maximum values of 0.17 dyn cm^{-2}, which is 7 times lower than values presented in literature (1.2 dyn cm^{-2} shear stress caused lethality within 12 h for E3.5 blastocysts [60] - Supp. Material Fig.S1).

The wide culture chamber and its consequent lower hydraulic resistance [61] prevent embryos being stressed by lethal WSS during the loading process. During fluid loading, the velocity profile in the inlet channel (hydraulic resistance in the order of 10^{10} Pa s m^{-1}) is significantly reduced in the culture chamber (where an evenly blue the outlet channel due to an increase in hydraulic resistance (~$10^{-12\text{-}13}$ Pa s m^{-1}). The inlet and outlet channels have similar fluid velocity profiles. The device was designed so that the total width of the outlet channels is comparable to the whole chamber width, thus the velocity profiles within the culture

chamber are optimized for embryo growth along the cross-sectional direction (Supp. Material Fig. S2).

An additional design criterion was used to favour the spreading out of the embryos across the whole culture chamber and to ensure a homogeneous perfusion of medium in the chamber. As shown in Fig. 2.C and in Supp. Material Fig. S2, a wide velocity profile of the optimized device design was obtained within the culture chamber along the cross-sectional direction when the device included multiple channels disposed parallel to the inlet channel. Real flow characterization performed by injecting fluorescein in the microfluidic chamber, showed that the green dye diffused and reaches equilibrium in 8 sec, as reported in Suppl. Materials Fig.S2.

As predicted from the computational analysis, the microfluidic device gave a flow profile as wide as the chamber width (Fig.2.C, Supplementary material, Figure S2). Considering the optimal diffusion of molecules and nutrients within the chamber (e.g. fluorescein) that this can provide, and the transient mechanical stimulation exerted on the embryos, these results suggest that embryos homogeneously spread in the chamber and receive equal amount of nutrient. Maintaining the embryos un-clustered but at close reciprocal distance favour paracrine signalling between embryos, and avoids detrimental accumulation of secreted products in the medium surrounding them.

After thawing and washing with fresh medium, 1 cell mouse zygotes were loaded in the device using a 145 µm pipette these pipettes are traditionally used for embryo culture and has a tip size compatible with the inlet port of the device. The embryos are manually injected into the inlet port and owing to fluid movement they safely move through the inlet channels and reach the central chamber (Suppl. Material Movie 1).

The microfluidic device was designed to minimize the clustering of embryos, even when cultured in larger groups of 20, 30 and 40 embryos.

Experiment 1. Blastocysts rate, hatching rates and outgrowth are not affected by the microfluidic environment. Assessment of morphology at distinct time points is regularly used for evaluating embryos' quality. Early cleavage, occurring on average at 24h after pronuclear fusion, has been correlated with embryo quality together with blastocyst rate and hatching rate both in mice and in human. Cryopreserved zygotes were thawed and cultured in potassium-supplemented Simplex Optimization Media (KSOM) in groups of 10 in standard 10 µL drops and in microfluidic devices. As summarized in Fig. 3, embryo development during microfluidic device culture was not altered when compared to traditional microdrop culture. Specifically, no significant differences were observed in cleavage rate, blastocyst rate or hatching rate.

Blastocyst adhesion competence *in vitro* was quantified by transferring embryos into fibronectin-coated plates for analysis of attachment and outgrowth formation (Fig. 3). This assay mimics the natural mechanism of adhesion of the blastocyst trophoblast cells onto the the endometrium which is regulated by interaction between the integrins naturally expressed on endometrial cells and on the apical surface of competent blastocysts [62-63]. By assessing the extension and adhesion of the hatched blastocysts it is possible to evaluate a mimic of their implantation potential. The blastocyst attachment data were similar between embryos grown in microfluidic device cultures (33.22 ± 5.6%, n=11 replicate cultures) and microdrop cultures (45.64 ± 8.4%, n=11 replicate cultures); these results were not statistically significant different from each other (p=0.35). Outgrowth rate, defined as the percentage of blastocysts forming outgrowths (18.2 ± 1.9%, n=11 vs control 30.6 ± 6.0%, n=11 replicate cultures, p=0.10) and mean diameter of the outgrowths formed were also not statistically different (144.5 ± 11.0µm, n=19 vs control 142.1 ± 9.0µm, n=19, p=0.72).

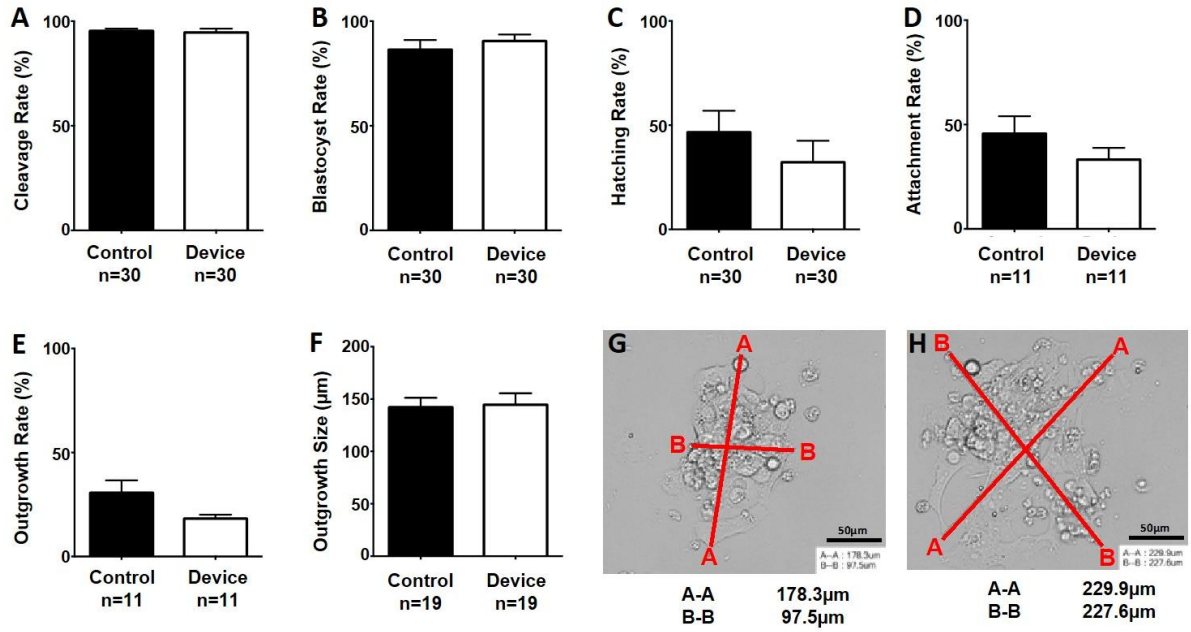

Figure 3: *Comparison of preimplantation embryo development. A) Cleavage rates (94.62 ± 1.7%, n=30 vs control 94.84 ± 1.08%, n=30, p=0.48). B) Blastocyst rates (out of total embryos cultured) (90.48 ± 3.2%, n=30 vs control 86.40 ± 4.6%, n=30, p=0.6), C) Hatching rates (out of total blastocysts) (32.18 ± 10.35%, n=30 vs control 46.61 ± 10.28%, n=30, p=0.32), D) Attachment rates (out of total blastocysts) (33.22 ± 5.6%, n=11 vs control 45.64 ± 8.4%, n=11, p=0.35), E) Outgrowth rates (out of total blastocysts) (18.2 ± 1.9%, n=11 vs control 30.6 ± 6.0%, n=11, p=0.08), F) Mean outgrowth size (µm) (144.5 ± 11.0 µm, n=19 vs control 142.1 ± 9.0 µm, n=19, p=0.72). Values plotted are means±sem for the number of embryos. G-H) Representative images of blastocyst outgrowth by embryos cultured in microdrops and microfluidic devices respectively: red lines indicate measurement bars created in RI viewer (A-A and B-B). Scale bar 50 µm.*

Cell number in a preimplantation embryo is directly correlated to the embryo health, developmental potential and ability for cell cycle progression. Total cell counts and cell allocation ratios in Day 7 blastocysts was carried out with an antibody-free differential staining method (Fig.4C) [64]. Total cell numbers were similar between controls and devices (Fig. 4A). There were also no significant differences between cell allocation to trophectoderm or inner cell mass lineages as expressed as percentage trophectoderm of total cells (Fig. 4B). The similar allocation and formation of the extra-embryonic cell lineage – trophectoderm and the inner cell mass (ICM) supports the negligible effect of the microfluidic confinement on embryo potency.

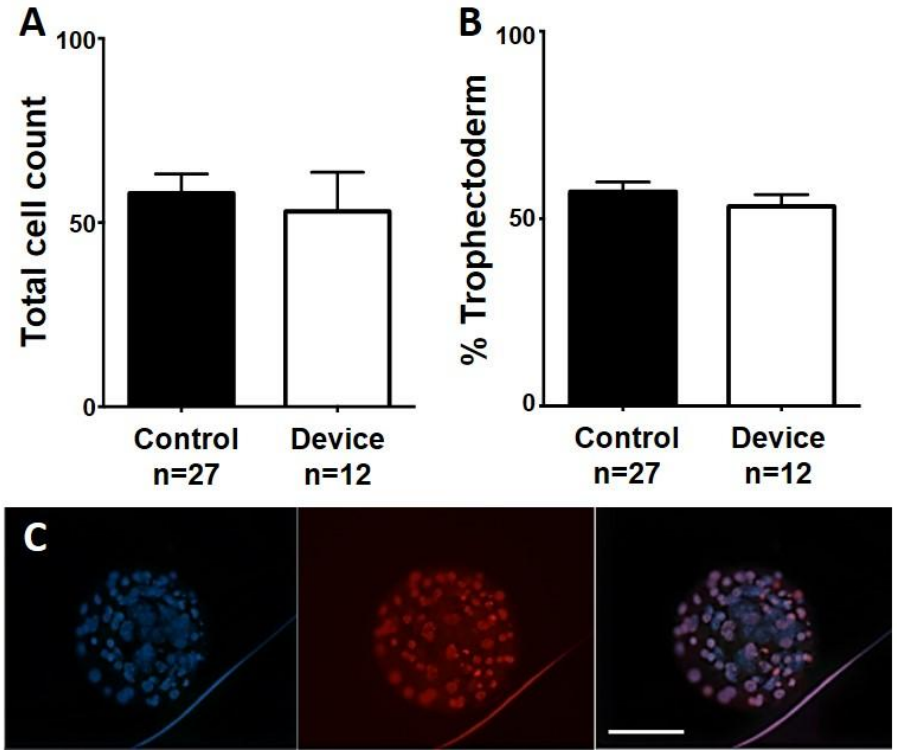

Figure 4. *A) Total cell count 53±10.6 cells, n=12 embryos, p=0.6 vs control 58± 5.2 cells, n=27 embryos. B) Cell allocation ratio (% Trophectoderm) 53.3±3.2%TE, n=12, p=0.4 vs control 57.2±2.6%TE, n=27, p=0.4. Values plotted are means±sem for the number of embryos analysed. C) Representative conventional epifluorescent image of blastocyst within the device stained with Hoechst 3342 and Propidium Iodide and imaged in the 460nm (blue) and 560nm (red) channels respectively. Scale bar 50 µm.*

Experiment 2. Embryo group size limits development and metabolic activity in the microfluidic chamber. The number of embryos cultured in a single microdrop and the volume of the microdrop are two variables that affect embryo development during culture. Different protocols have been compared to identify an optimal range of embryo density, in terms of µL of medium available per embryo. In a microfluidic system, the embryos are confined in a different environment, specifically a 400 nL static chamber is linked through two side channels and allows two 10 µL drops of medium to be available to provide nutrients during ~3 days of culture. It is extremely important to evaluate how the different fluidic environment can support embryo growth and provide sufficient nutrients.

When comparing groups of 10, 20, 30 and 40 embryos grown in the microfluidic device, due to the variability of the data the overall blastocyst rate was not significantly different between groups of different size (p=0.25) (Fig. 5). That said blastocyst rates were highest in the device 10x group, and decreased with the size of the group, from ~90% in the 10x group down to ~56% for the larger group of 40 embryos. Groups of 10 embryos very consistently gave 80-90% blastocyst rates, while larger group sizes were very variable between replicate cultures. In marked contrast, hatching rate in devices significantly decreased with increased group size (10x group: 30±4% compared to 40x group: 2.2±2%, n=4, p=0.02). This suggests that substrate competition outweighs increased paracrine effects in larger group sizes.

Development rates are a widely used key marker of ongoing developmental competence. However, to examine embryo competence in richer detail, metabolic parameters were investigated. Blastocysts were labelled and imaged directly within the devices using the ratiometric mitochondrial dye JC-10 (Fig. 5) to evaluate changes in mitochondrial membrane potential. JC-10 accumulates in the matrix of polarised mitochondria, forming J-aggregates

with punctate red fluorescent signal. In areas of reduced mitochondrial polarisation, the dye tends to remain in monomeric form with diffuse, green signal. Mitochondrial polarisation thus indicates overall mitochondrial polarisation in mammalian oocytes and embryos [64]. Control blastocysts cultured in microdrops did not have a significantly different mitochondrial polarisation ratio (0.64±0.02, $p>0.92$) compared to device-cultured embryos, regardless of the groups size. However, following device culture, blastocyst polarisation ratio was significantly higher in 10x groups (0.67±0.04, n=27) compared to 20x groups (0.62±0.01, n=42, p=0.01) 30x groups (0.61±0.07, n=71, p=0.0005) and 40x groups (0.61±0.7, n=66, p=0.001). Overall blastocyst mitochondrial polarisation ratio correlated strongly with blastocyst rate across all groups (p=0.01), confirming the viable status of the embryos.

Control embryos had metabolic profiles typical of microdrop-cultured murine blastocysts [44,45, 65, 66]. Device-cultured embryo pyruvate and glucose consumption decreased with increasing group size. Embryos cultured in groups of 40 had significantly reduced pyruvate (0.37±0.1 pmol/embryo/hr) and glucose consumption (0.05±0.03 pmol/embryo/hr) than groups of 10 (1.4±0.08 pmol/embryo/hr, and 0.8±0.08 pmol/embryo/hr, respectively p=0.02). Pyruvate is the preferred energy substrate during early cleavage, while glucose consumption is low during early cleavage but tends to increase greatly with increased ATP generation through oxidative phosphorylation at the blastocyst stage [45]. The present data suggests increased competition for these substrates within the more concentrated population of 40 embryos in comparison to groups of 10 in either devices of control microdrops. Device embryos were more quiescent overall, with reduced variation between culture groups. Embryos with metabolic profiles in the intermediate or *lagom* range and with a tighter distribution may be the most developmentally viable, due to undergoing less metabolic stress [45]. The minimal, physiologically accurate volume of available medium in device culture may encourage embryos towards this moderate metabolic profile and improve embryo developmental potential.

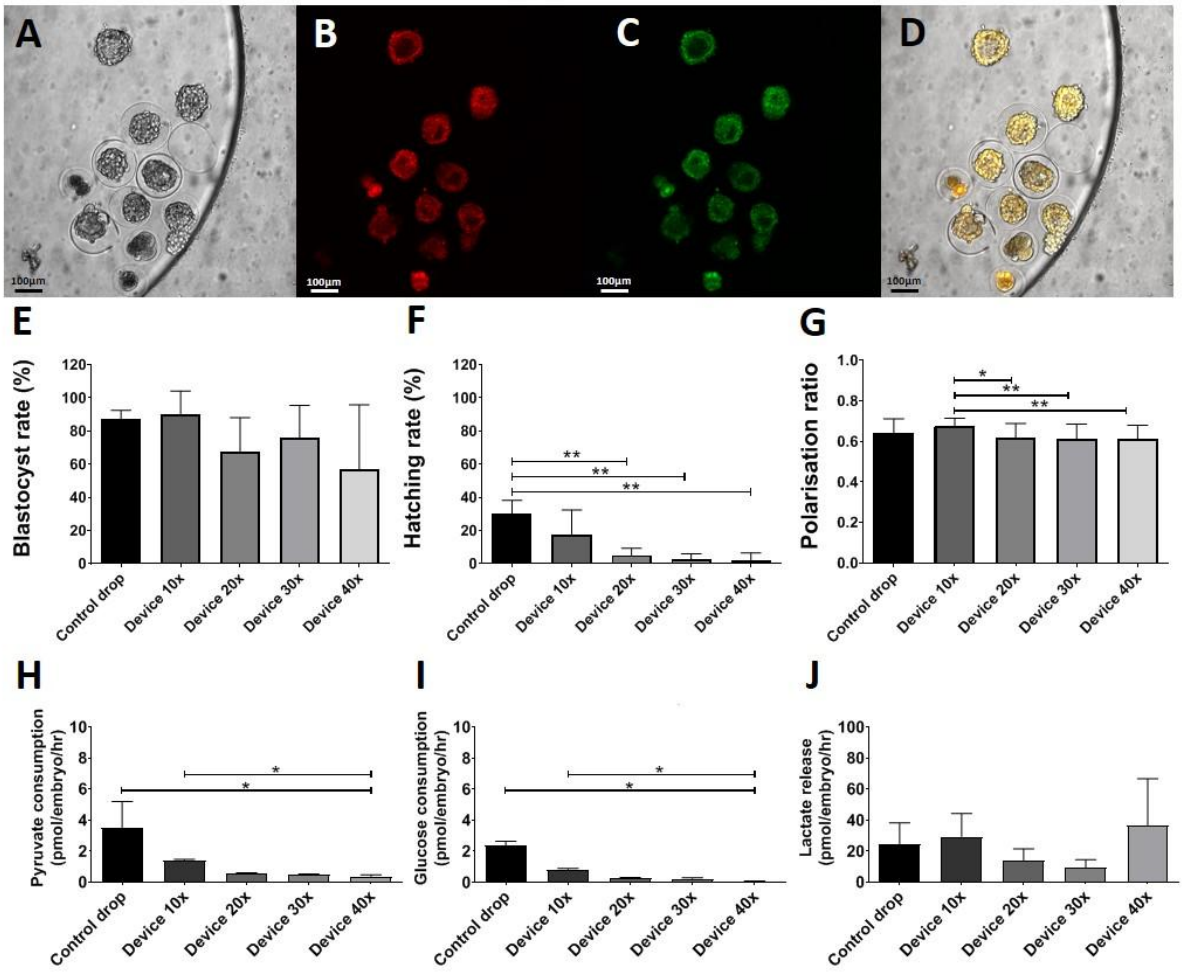

Figure 5. *Loading capacity experiment. A) Brightfield, B-D) Analysis of mitochondrial polarisation ratio. Representative conventional epifluorescent images of blastocysts within the device stained with the potentiometric mitochondria-specific stain JC-10 and imaged in the rhodamine isothiocyanate (RITC, B) and fluorescein isothiocyanate (FITC, C) channels respectively. Scale bar 100 µm. E) Blastocyst rate (n=4) F) Hatching rate (n=4) G). Quantified blastocyst polarisation ratio data (n=4) shows higher value when culturing groups of 10 embryos inside the device. H-J) Energy substrate turnover (n=4).the 5 replicate cultures. *indicates significant differences at P<0.05.*

Experiment 3. Microfluidic confinement does not affect development and implantation related gene expression. Using Real-time PCR (qPCR) of single blastocysts, the expression of a panel of 53 genes involved in blastocyst development and cell differentiation was analyzed (Supporting Material, Table S1). Overall, the gene expression profile of murine blastocysts cultured in the microfluidic device is similar to that observed in blastocysts cultured in traditional microdrops (Fig. 6). Exceptions include the imprinted gene *Xist* and *Sbno1* which resulted highly expressed in the device group ($p > 0.05$) compared to the microdrops group. *Xist* is known to have a role in the X chromosome inactivation [67], whereas *Sbno1* [68] expression is fundamental for murine blastocyst development and involved in trophectoderm differentiation. An increase in expression of those genes could be linked to beneficial effects of the microfluidic device on embryo development. However, further analysis is needed to confirm these findings and to measure absolute gene expression levels for comparison with previously publishes studies. Additionally, differential expression of marker genes involved in

trophectoderm differentiation (*Klf5* [69], *Cdx2* [70], *Tead4* [54], *Gata* [70], *Elf5* [55], *Krt18* [53]) or ICM/epiblast development (*Stat3* [71], *Nanog* [52,53,73], *Pou5f1* [71], *Sall4* [72], *Gata6* [73]) was measured (Supporting Material, Fig S3). Due to the variability of the data no statistically significant differences were observed in these genes when blastocysts developed in the microfluidic device were compared to those cultured in traditional microdrops. These results could be further validated by increasing the sample size (i.e., number of expanded blastocysts for each experimental group) and by exploring the effect of each specific genetic alteration on embryo function and development.

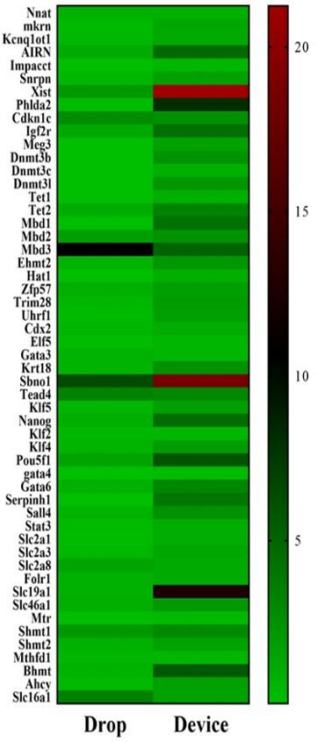

Figure 6. *Heatmap representing gene expression of mouse blastocysts cultured in the device compared to microdrop culture. Scale: red indicates high expression and green is low expression.*

Experiment 4. PDMS alters the medium composition but does not induce drastic changes in the embryo metabolism. Global, untargeted liquid chromatography tandem mass spectrometry (LC-MS/MS) analyses were performed to compare spent medium (KSOM) on days 4 or 5 of embryo culture between each experimental groups: KSOM, KSOM + microdrop, and KSOM + device. The metabolite composition of spent KSOM collected from the microfluidic device was compared with that of spent medium collected from control microdrops, both in the presence or absence of embryos (n= 3 replicate cultures for each treatment group). The Principal Component Analysis (Fig. 7A) and heatmap (Fig. 7B and Fig. S4) show distinct clustering of the experimental groups. These global views revealed that while the majority of the detected metabolites were stable and present in abundance, there was a modest subset of metabolites in culture medium with unique abundance profiles between device and microdrop culture methods.

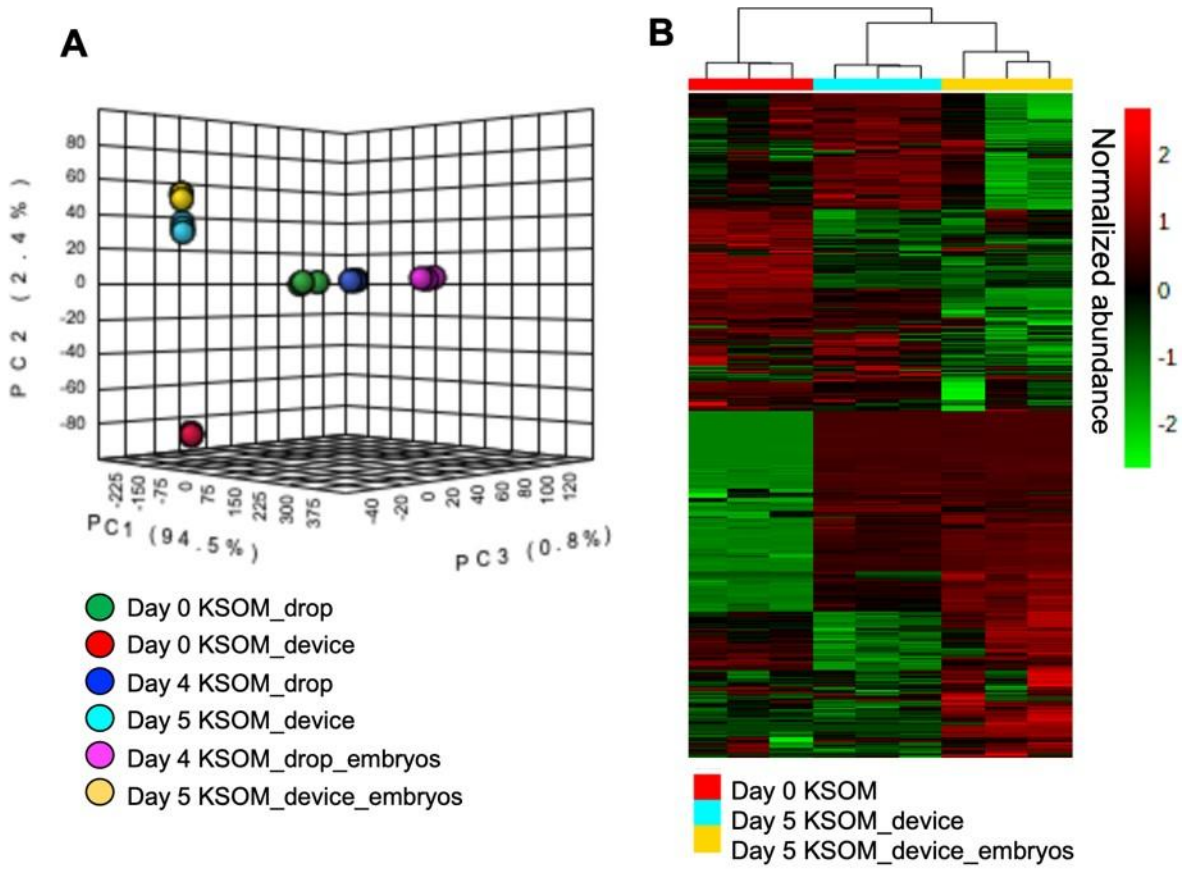

Figure 7. *Principal Component Analysis (PCA) and heatmap visualization of global, untargeted mass spectrometry. (A) PCA plot of the LC-MS/MS data of medium samples from devices after 4 days in microdrops or 5 days in devices and control KSOM (n=3 replicate cultures per experimental group). (B) Heatmap analysis of media samples collected from the microfluidic device with and without embryos. Sample replicates are visualized in columns column based on hierarchical clustering, with metabolites presented on individual rows. Species are colored based on normalized abundance from red (high) to green (low).*

Second-order meta-analysis of the individual pairwise comparisons (Fig. 8) allowed prioritization of endogenous or xenobiotic compounds (specific to PDMS, PS or mineral oil exposure) that were altered in abundance by the embryo culture method (device vs. microdrops). The Venn diagram shows shared and unique compounds for specific comparisons. A comparison of the compounds identified in spent media from devices ("PDMS-media") or spent media from control microdrops cultured in a standard Polystyrene dish ("PS-media") without the presence of embryos revealed a total of 547 compounds (Fig. 8A). Using meta-analysis, 48 compounds were common to the 2 groups (device vs. microdrop), whereas 387 were unique to the PDMS-media group and 64 to the PS-media group. Compounds unique to the device group, represent xenobiotic species directly associated with PDMS use. These data show 339 xenobiotic compounds were released by PDMS into the culture medium and 48 compounds were absorbed by- or adsorbed onto- the PDMS from the culture medium. The 339 species released into the culture medium, included detection of plasticizers such as butyl lactate, dimethyl sulfoxide, ethanol, 2-[2-(2-butoxyethoxy)ethoxy]-, N,N-dimethylformamide, necatorine, pentaethylene glycol, triethylene glycol and tripropylene glycol. The effects of these potentially toxic compounds on embryo development must to be further investigated. The remaining compounds detected indicate breakdown products of media components produced by media degradation over 5 days of incubation at 37 °C. These

include peptides, amino acids and other small endogenous molecules (e.g., l-glutamine, l-tryptophan, n-phenylacetylglutamic acid, pyridoxamine, dihydrolipoamide).

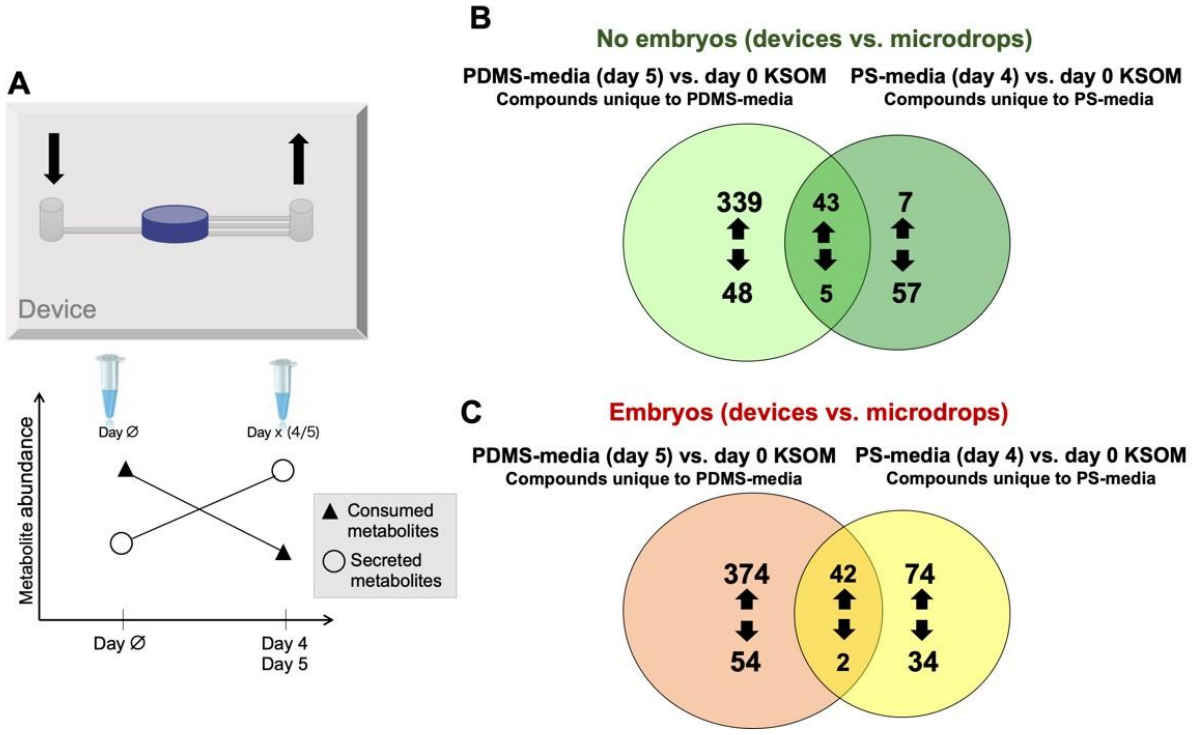

Figure 8. *Venn diagram of dysregulated compounds in PDMS-media and PS-media compared to control (day 0 KSOM). (A) Schematic of the device with arrows indicating inlet (↓) and outlet (↑) ports (top). Changes in metabolite abundance in samples collected from microdrops (day 4) or devices (day 5) when compared to control. Increased and decreased compounds represent, respectively, released and consumed metabolites (bottom). (B) Comparison of dysregulated compounds in day 5 PDMS-media and day 4 PS-media without embryos. (C) Comparison of dysregulated compounds in day 5 embryo culture PDMS-media and day 4 embryo culture PS-media.*

Similarly, among the 48 species that were significantly decreased in spent media from the device (Fig. 8A), numerous biological compounds were identified that were sequestered by PDMS from the culture medium, these include: amino acids and dipeptides (e.g., isoleucyl-isoleucine, isoleucyl-leucine, isoleucyl-phenylalanine, n-acetyl-l-methionine, and valyl-leucine).

Among the species that were significantly decreased (57 compounds) in spent media from microdrop culture, peptides and amino acids, such as L-tyrosine, aspartylphenylalanine and phenylacetylglycine were identified. These data suggest that these molecules were absorbed or transformed by the plastic or mineral oil. The remaining detected compounds represent breakdown products of culture media that degraded over time.

Other organic species appeared down-regulated in PS-media and PDMS media suggesting a segregation of compounds from the medium both into the elastomer as well as in the plastic or the mineral oil used to prevent media evaporation. These molecules included tryptophol [xylosyl-(1->6)-glucoside], muramic acid, [3,5-dihydroxy-2-(hydroxymethyl)-6-[3,5,7-trihydroxy-2-(2,4,5-trihydroxyphenyl)-3,4-dihydro-2H-1-benzopyran-6-yl]oxan-4-yl]oxidane-sulfonic, and 2-methoxyestrone 3-glucuronide.

Subsequently, a second-order meta-analysis of spent media collected with embryos present in the device and in the microdrop method was performed. Specifically, embryo cultured spent media from devices (day 5) were compared to embryo present spent media from microdrops (control, day 4) (Fig.8B). These analyses allow for us to determine metabolites and/or

xenobiotics present in spent media after embryo culture (i.e., produced or consumed by the embryo during culture) as well as xenobiotics unique to device culture (i.e., associated with the fabrication process or released/absorbed by PDMS) or to control microdrop culture (i.e., associated with PS or the mineral oil used to prevent medium evaporation). The Venn diagram shows 428 species to only be present in embryo cultured PDMS-media, 108 compounds were only observed in embryo culture PS-media and 44 species were present in both embryo culture PDMS-media and embryo culture PS-media (Fig. 8B).

Putative metabolite identifications were used for pathway overrepresentation analysis using Metaboanalyst 4.0. From the comparison of the media from the device and the control culture in polystyrene dishes at the end of the culture, it was possible to identify 374 significant compounds uniquely up-regulated in day 5 embryo culture PDMS-media. The view map in Fig. 9A revealed that the most significant enriched pathways for these metabolites were tryptophan metabolism, arginine biosynthesis, pantothenate and CoA biosynthesis, and cysteine and methionine metabolisms. Similarly, Fig. 9B presents a list of the matched overrepresented pathways for the 74 significant compounds uniquely up-regulated in day 4 embryo culture PS-media. The metabolome view revealed that the most significant enriched pathways for these metabolites were terpenoid backbone metabolism, arginine biosynthesis, and arginine and proline metabolisms. Thus, the culture environment provided by the microfluidic system had a significant impact on some metabolic pathways (i.e., amino acid metabolism), although further assessment of its role on mouse embryo development and implantation potential need to be investigated.

The complete lists of metabolites used for the presented pathways overrepresentation analyses are provided in Table S2 and Table S3.

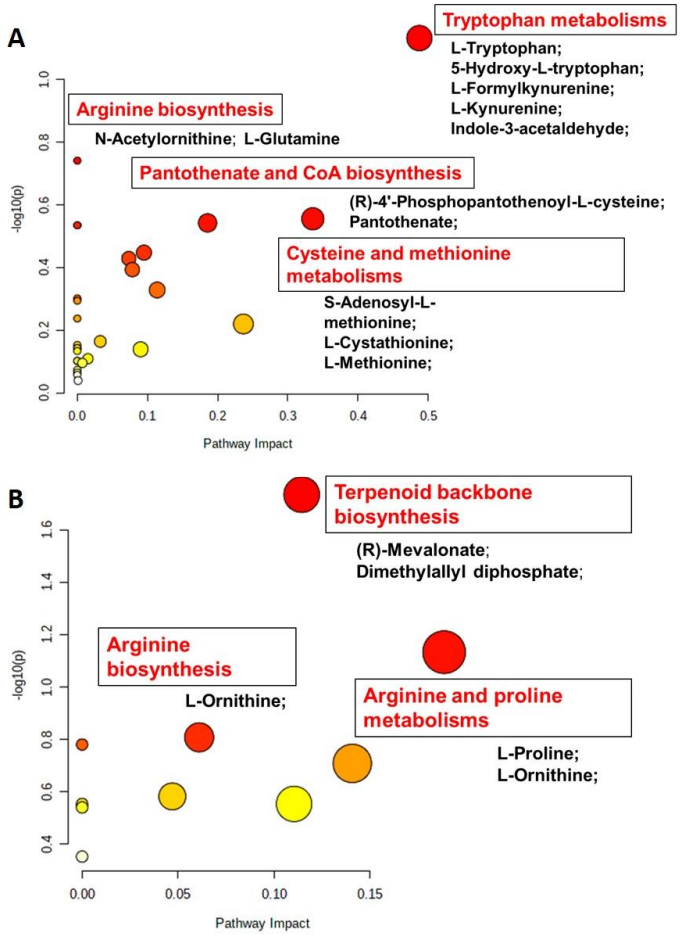

***Figure 9**. Pathways overrepresentation analysis. Summary of metabolic pathways of significant metabolites uniquely up-regulated in day 5 embryo culture PDMS-media (vs. day 0 KSOM) (A) and in day 4 embryo culture PS-media (vs. day 0 KSOM) (B). The metabolome view contains results of the analysis generated by Metaboanalyst with all the matched pathways arranged by p-values on Y-axis, and pathway impact values on X-axis.*

Notably, among the 44 common metabolites present in both embryo culture PDMS-media and embryo culture PS-media, the relative abundance of 42 of these compounds were statistically significantly increased ($p<0.05$ and fold change ratios > 2) in both media when compared to control, these identified compounds include metabolic markers of pre-implantation embryo development, such as pyroglutamic acid, 5'-methylthioadenosine [74], hypoxanthine [75-76], cytosine, n-acetyl-l-methionine, and phenylacetylglycine. Pre-implantation embryo development compounds represent metabolites produced by embryos in both culture conditions. Similarly, 2 compounds significantly decreased in spent embryo culture media compared to control (i.e., muramic acid and meticillin) might be consumed by embryos from the culture medium.

In summary, these results allow us to conlcude that metabolomic changes could be detected by mass spectrometric analysis in samples of media collected during embryo culture, and these were correlated with organic and inorganic compounds available to the embryos during their development *in vitro*.

Discussion

The novel microfluidic device we have designed and fabricated in PDMS, provided a simple and user-friendly system for culturing groups of murine embryos and enabled the use of several, non-invasive techniques for assessing embryo quality. The device was designed for optimal embryo loading of 10-12 embryos per device. The data indicated that the individual microfluidic compartments of the device permitted user friendly, efficient and reproducible loading and retrieval of the embryos. The microfluidic device and culture strategy was conducted in the absence of oil and served to demonstrate the compatibility of our device with standard bench top incubators and optical microscopes.

Mouse embryos grown in our microfluidic devices under optimised loading conditions demonstrated similar developmental capacity to embryos derived using the widely adopted microdrop culture method, with both cleavage and blastocyst rates exceeding 90% in all culture conditions. The evidence presented clearly demonstrates that if the optimal loading capacity of the device is exceeded then nutrient depletion and metabolic stress is induced which impacts severely on embryo health and developmental potential as indicated by the reduced capacity for microfluidic-derived embryos to metabolise glucose and to hatch relative to controls. Under optimal loading conditions, microfluidic device culture had no impact on blastocyst cell number and blastomere partitioning between the ICM and TE. Furthermore the blastocysts grown in microfluidic devices demonstrated equivalent capacity for hatching and out growth *in vitro*, factors which are indicative of implantation potential *in vivo* [77]. Taken together, these data indicate that the novel microfluidic device presented here is embryo-compatible and can successfully be used to support healthy embryo development to the blastocyst stage without the need for media changes or oil overlay.

The analysis of gene expression of single blastocysts derived in the microfluidic device provided a clear assessment of the influence of the microfluidic confinement on the embryo quality. The selection of genes correlated to the preimplantation and endometrial receptivity provides evidence to support limited alterations of the embryos during the 5 days of culture.

However, in this work gene expression levels were measured using relative quantification method, which did not allow to obtain information on the absolute expression value for each gene. Further analyses might use absolute quantification methods to measure expression

levels of selected genes, to directly compare our findings with available gene expression datasets and elucidate specific impact of the gene alteration on embryo culture. Moreover, qPCR data will also be validated by increasing sample size, i.e., the number of analyzed blastocysts for each experimental group, to provide further evidence on the impact of altered expression of key genes in embryo development and implantation potential. A particular focus will be addressed to metabolic and epigenetics markers to more deeply investigate the impact of microfluidic culture.

The combination of gene and metabolite data analyses are complementary, metabolomics data allows us to identify at the molecular level metabolites released by the embryo or consumed by the embryo during development while genomic data allows us to follow changes of embryo development at the gene and protein level. Interestingly, the cultured medium is altered significantly at day 0, in accordance with previous work on PDMS absorption [78] and the release of xenobiotic compounds in the medium is present in a few hours. These compounds can be ascribed to the unstable hydrophilic properties of the PDMS over time. These properties influence leaching and sequestration of small molecules by the elastomer [79]. As revealed by the culture medium analysis, specific compounds can be found uniquely in the samples derived from the microfluidic system. In these data, numerous uncrossed-linked components of the PDMS were identified. Second-order meta-analysis allowed for biologically important metabolite changes to be observed in the culture medium throughout embryo development. Pathways overrepresentation analysis showed that microfluidic culture had a significant impact on tryptophan metabolism pathway, which could explain the resulting activity of protein synthesis mechanisms fundamental during embryo development. Importantly, MS data did not reveal alteration of metabolites involved in metabolic pathways of glucose, pyruvate and lactate. This suggests that the microfluidic environment does not alter energy substrate metabolism, as also shown by our metabolic profile data (Fig. 5H-J). Similarly, no significant changes in abundance of metabolites involved in oxidative stress processes were detected from the analysed datasets, which demonstrates that the plastic does not impact the release of reactive oxygen species into the culture media. Identification and quantification of metabolite and xenobiotic compounds is not completed at this stage, however these data show that the presence of the embryo in culture altered the composition of the medium in the device and in the microdrop method. These data also show that the number of common compounds in the different culture settings (device vs. microdrops) were changed. However, under optimal loading conditions the embryos developed successfully in the PDMS device, without significant alterations. The stability of PDMS may represent a challenge in the field of microfluidics and lab-on-chip research, however alternative plastics for manufacturing of the device could be used for this novel system. The methods used for evaluating the embryo development in this work should be performed at minimum for industrial manufacturing plastic. Importantly, from the morphokinetic analysis, these unexpected xenobiotic compounds observed in the medium did not induce significant alteration of the embryo development at different stages.

Oxygen availability is also a key requirement for embryo development [80]. In this work, we assessed the effect of the confinement of the embryos in a close compartment, completely surrounded by PDMS, which is permeable to gas [81-82]. Oxygen tension of 5% for embryo culture has been widely adopted in both animal and clinical human IVF laboratories and considered a more physiological concentration that can boosts blastocyst development with no detectable adverse effects [83-85]. While it is true that the diffusion of oxygen through the PDMS could be modelled and compared to that through mineral oil and media, with optimal embryo loading we did not observe detrimental effects on the embryo development due to a different oxygen dynamic.

The microfluidic device culture facilitated harvesting of individual blastocysts for analysis of specific genetic profiles by real time qPCR. In this study the relative expression of 53 specific genes involved in blastocyst development and cell differentiation, trophoblast and epiblast development, aimed to exclude any genetic alteration induced by the microfluidic environment.

In order to use the same technique and to correlate those specific genes to the blastocyst competence, a more consistent breeding protocol would be required, with standardization of fertilization method, sperm and egg donor and including different mouse strains.

The LC-MS/MS analysis of spent media revealed changes in the media composition, with sequestration of molecules and different consumption and release of compounds by the embryo in the microfluidic device and in the standard microdrop method. These data improve our understanding of the embryo metabolic activity and confirm the unstable characteristics of the prototyping elastomer. A more detailed analysis could be set up by collecting samples every 2 hours to correlate altered media composition with abnormal embryo developmental rates to morula or blastocyst stage. Future analyses of the medium composition will be used to search for specific toxins, such as peroxides derived from the mineral oil, zinc, and other unknown contaminants that may be released into the medium from the oil or the plastic. Despite, the presented study provides valuable information of genetic and metabolic alterations induced *in vitro* by the culture environment, the presented data might be significantly improved by increasing sample size and number of experimental replicates. Importantly, further investigation are required to correlate the observed alteration in gene expression with metabolite changes and specific pathways affected by the different culture environment, with a particular interest on oxidative stress and metabolic activity.

Finally, the data presented show the feasibility of performing both PCR and metabolomics analyses from single stage matched blastocysts. The gene expression data generated from the microfluidic device shows the capability of profiling of preimplantation embryos in a microfluidic environment and confirms the impact microfluidic technology has in fundamental research in assistive reproductive technology. Further investigations are needed to explore the effects of device culture on embryo implantation and live birth rates. Embryo transfers in mice and assessment of birth rates will confirm the competence of embryos cultured in the microfluidic device and will allow to quantify time and costs saving introduced by this protocol. Preliminary data gathered so far on embryo transfer with BL6 mice [86] has shown improved birth rates (53%) when transferring embryos cultured for 48hrs in the devices with surgical procedures. When combined with NSET, the microfluidic culture ensured successful implantation of *in vitro* matured blastocysts (success rate >25%). Further trials are now planned to evaluate the improvement in terms of birth rate, including different strains of the recipient mice, cryopreserved or fresh embryos and using specific protocols for embryo transfer.

This novel microfluidic technology eliminates the current standard use of potentially toxic mineral oil for embryo culture, thus reducing toxicity, failure, and costs for each culture set up. The loading and retrieval are significantly simplified compared to the microdrop technique, allowing to pipette an entire group of 10 embryos in a single step. This represents an additional value in high throughout facilities to maximize the costs and the success of the culture. More importantly this new method also favours the adoption of NSET. Furthermore, the device characteristics can be revised and easily adapted to host larger animals (e.g. bovine, equine) and human embryos. This data set thus represents a first step towards to development of a new solution to improve the efficiency of human embryo culture during assisted conception treatment. The compatibility with the most advanced methods for assessing material toxicity and embryo quality will be key to correctly assess the safety and the performance of this new device.

Materials and methods

Microfluidic device flow and shear stress analysis.

All chemicals were purchased from Sigma Aldrich (St Louis, MO, USA) unless specified otherwise. COMSOL Multiphysics 5.2a was used to evaluate and compare flow rate, velocity

field and predict shear stress as function of microfluidic device geometry. To generate a 3D model, the microfluidic design was first created by using computer-aided design software (Autodesk AutoCAD 2017). The design geometry was then imported into a COMSOL library. The fluid inside the device was simulated as an incompressible, homogeneous, Newtonian fluid with density (ρ=1000 kg m^{-3}) and viscosity (μ=1x10^{-3} Pa s) [81]. Flow was created by manually loading a solution of 4.8 µm fluorescent polystyrene beads using an embryo handling Flexipette with 170µm tip (EZ-Grip, RI, Cooper Surgical, Denmark). The maximal velocity in the inlet channel was estimated to be respectively about 0.4 mm s^{-1}(as average of 10 measurements) which corresponds to a flow rate equal to 1.17 µl min^{-1} (Re: 0.087). The devices showed a widely lower flow rate compared to the theoretically derived harmful value previously calculated (13.91 µl min^{-1}).The estimated inlet velocity was applied to a COMSOL model to predict the shear stress the device during embryo loading (Suppl. mat., Figure S1). Critical values of shear stress (~3.5 dyn cm^{-2}) were only found on the edges at the interface between culture chamber and outlet channels, areas that embryos cannot reach because of the narrow outlet channels section.

Once velocity has been assessed, to prove the computational model results and to better characterize flow profile inside the microfluidic chambers a solution of fluorescein (0.05 mg ml^{-1}) was flowed into the chamber previously filled with water.

Microfluidic device fabrication and preparation for culture.

Microfluidic devices were fabricated in polydimethylsiloxane (PDMS, Sylgard® 184, Dow Corning, MI, USA). This microfluidic structure was obtained by bonding together two layers of PDMS (Figure 1. B), where microchambers and microchannels are defined by standard soft lithography techniques. Once assembled, the devices were immediately filled with sterile tissue culture water and stored closed at 4°C to preserve hydrophilicity. Before embryo culture, devices were sterilized by exposure to UV light (254 nm wavelength for 30 minutes). Devices were then prepared by drawing 10µl KSOMaa (Millipore, UK) from the inlet through the channel and chamber. Devices were then primed by overnight incubation with 10µl KSOMaa media drops added to the inlet and outlet ports in a benchtop MINC™ Mini incubator (Cook, Aus) at 37 °C in humidified 5% CO_2, 5% O_2, 90% N_2. The microfluidic devices were placed inside 60 mm culture dishes and surrounded with embryo tested sterile water. To load embryos, embryos were placed in the inlet chamber and media was drawn through from the channel outlet until all embryos entered the central chamber (Supplementary material, Video 1 Loading and Video 2 Retrieval). 10µl drops of pre-equilibrated KSOM were then added to channel inlet and outlet before culture at 37 °C under 5% CO_2, 5% O_2 in humidified nitrogen.

A total of 46 devices were used for embryo culture in experiments 1 and 2 and additional 30 devices for RT-PCR and metabolomic analysis in experiments 3 and 4.

***In vitro* embryo culture in microdrops.**

Cryopreserved embryos (strain C57BL/6N) for Experiment 1 and 2 were supplied at zygote and 2-cell stages by MRC Harwell, UK. 1-cell murine embryos (B6C3F1xB6D2F1 strain, EmbryoTech, USA) were used for experiments 3 and 4. On the first day of culture, murine presumptive zygotes were thawed following established protocols. Briefly, embryo straws were held in air for 30s, then plunged into room temperature water until the contents had visibly thawed (around 10s). The straws were cut at the seal and the plug bisected before pushing the contents into a 60 mm IVF hydrophobic culture dish. Embryos were incubated for 5 min before 2, 5 min washes in 100µl M2 medium at 37 °C. Embryos were then washed through 3, 500µl wells of pre-equilibrated KSOMaa before transfer to devices or culture microdrops. Culture microdrops were 1µl/embryo in 35mm hydrophobic IVF certified dishes (Nunc), covered with 5 mL of BioUltra mineral oil from Sigma Aldrich.

Experiment 1- Cell count, outgrowth assay.

A total of 60 embryos were cultured in microdrops and microfluidic devices in a series of 5 replicate cultures. Cell counts at the end of culture were performed using the method described by Thouas et al. [45]. Briefly zona-intact blastocysts were first incubated in 500µL of Dulbeccos PBS with 1% Triton X-100 and 100µg/mL propidium iodide for 5s resulting in a labelled trophectoderm with red fluorescent signal. Blastocysts were then immediately transferred into 500µl of fixative solution (100% ethanol with 25 µg/ml Hoechst 33258) and stored at 4°C overnight. Fixed and stained blastocysts were then mounted onto a glass microscope slide and gently flattened with a coverslip to facilitate the individual identification and counting of fluorescent cells. Fluorescent images were taken on a Zeiss AX1 Epifluorescence microscope and analysed in ImageJ.

Outgrowth assays were performed as described by Hannan et al. [87]. Blastocysts were imaged and measured using a Nikon ICSI microscope with RI viewer software.

Experiment 2 – Blastocyst rates, energy substrate consumption and mitochondrial polarization.

To define the loading capacity of device culture, groups of 10, 20, 30 and 40 2-cell mouse embryos were cultured to the blastocyst stage in microfluidic devices in parallel to controls (10 embryos in one 10 µL culture microdrop) before metabolic profiling. A total of 220 blastocysts were analysed in each treatment group from 5 replicate cultures.

Glucose and pyruvate consumption were measured using spent media from devices or microdrops by the method of Guerif et al. [44] and expressed as mean pmol/embryo/hr ± SEM. Briefly, 10µl of reaction mixture was added to the base of a black 384 well microplate. 1µl of spent media from each device or microdrop was added to each reaction mixture well and the difference in NAD, NADH or NADP signal, measured at 340/460nm, was calculated. Concentrations were calculated using a 6-point standard curve and expressed in terms of pmol/embryo/hr.

Day 5 blastocysts were labelled and imaged within devices using the ratiometric mitochondrial dye JC-10 (Molecular Probes). Briefly, a 1mg ml^{-1} JC-10 stock solution was prepared in KSOM culture media. JC-10 stock was diluted to 10µg/ml in pre-equilibrated M2 media (Millipore). Following removal of spent media for energy substrate assays, media was replaced with this JC-10 solution and incubated at 37 °C for 30 min. Control embryos were imaged on glass slides, while device embryos were imaged within devices to avoid stress. Imaging was performed on a LSM 780 confocal microscope, while image analysis was carried out in ImageJ. Data was represented as red fluorescence/total red+green fluorescence to account for any non-specific fluorescence across both channels. Higher values indicate a higher level of mitochondrial polarisation throughout the measured region of interest.

Experiment 3 - Real-time PCR (qPCR) of single blastocysts.

Groups of 10, 1-cell murine embryos were cultured in KSOM medium in 10µl microdrops (control) and inside the devices. 90 blastocysts were analysed in each treatment group from 3 replicate cultures. Individual, stage matched, expanded blastocysts were recovered from devices or control microdrops, and immediately transferred into 2µl RNAGEM lysis buffer (RNAGEM Tissue Plus®, MicroGem International PLC, Southampton, UK) and frozen at -80°C. For the construction of cDNA libraries of individual blastocysts we modified an existing protocol [88]. In summary, total RNA from single blastocysts was isolated using an RNAGEM-extraction reagent mastermix. The total RNA was reverse-transcribed to cDNA using a first strand cDNA synthesis kit (Thermo Fisher Scientific Inc., UK). Quantitative PCR (qPCR) was performed on 6-fold diluted sample cDNA to analyse expression of 53 selected genes associated with blastocyst development and cell differentiation. Accession number, primer sequence and product length of target genes are presented in Table S1. Ten individual

blastocysts were analyzed in each experimental group. mRNA expression was examined using SYBR Green Master PCR mastermix (Thermo Fisher Scientific Inc., UK) with an ABI 7500 RT-PCR System (Applied Biosystems) over 40 cycles and using the house keeping genes listed in Table 1. Data were analysed with 7500 Software using relative quantification analysis.

***Table 1**. Summary of gene symbol, accession number, product length and primer sequences of the housekeeping genes.*

Symbol	Name	Accession	Size (bp)	Sequence of nucleotides (5'→3')	
Eif1	Eukaryotic translation initiation factor 1	NM_011508	186	Forward	AAGGGCTACCTTTCCAGAGA
				Reverse	GCACTGGCTCGTACTGAGTT
Rpl13a	Ribosomal protein L13A	BC086896	215	Forward	ATGACAAGAAAAAGCGGATG
				Reverse	CTTTTCTGCCTGTTTCCGTA
Gapdh	Glyceraldehyde-3-phosphate dehydrogenase	BC083080.1	223	Forward	CTGGAGAAACCTGCCAAGTA
				Reverse	TGTTGCTGTAGCCGTATTCA
Rplp0	Ribosomal protein, large, P0	NM_007475	202	Forward	AACCCAGCTCTGGAGAAACT
				Reverse	GGAAGAAGGAGGTCTTCTCG
Ywhaz	Tyrosine 3-monooxygenase/ tryptophan 5-monooxygenase activation protein, zeta polypeptide	NM_011740	181	Forward	AGCAGGCAGAGCGATATGAT
				Reverse	TTCTCAGCACCTTCCGTCTT
Actb	Actin, beta	NM_007393	160	Forward	AAGAGCTATGAGCTGCCTGA
				Reverse	TACGGATGTCAACGTCACAC
18s	18s ribosomal RNA	NR_003278	298	Forward	ATTCCGATAACGAACGAGACT
				Reverse	AGCTTATGACCCGCACTTACT
Pgk1	Phosphoglycerate kinase 1	NM_008828	185	Forward	GCAGATTGTTTGGAATGGTC
				Reverse	TGCTCACATGGCTGACTTTA

Experiment 4 - Global untargeted metabolomics

To investigate impact of microfluidic culture on the embryo secretome and to establish if the PDMS matrix released low molecular weight species or sequestered hydrophobic biomolecules from culture media [89], we analysed and compared samples of spent media (KSOM) collected from devices to samples of spent media collected from control KSOM microdrops cultured with and without embryos using global untargeted metabolomics. 1-c murine embryos were cultured using the same embryo-to-volume ratio in microdrops or PDMS devices. Specifically, groups of 10, IC zygotes were cultured in either 40μl KSOM microdrops under oil or in each microfluidic device, where 20μl drops of media were added to each inlet and outlet ports. Samples were collected from microdrops and microfluidic devices when embryo development had progressed to the fully expanded blastocyst stage, to allow stage-matched comparison of embryo metabolite production/consumption. Specific to this study, the blastocyst stage was achieved at day 4 in microdrops and day 5 in devices. Samples of spent media (40μl) were collected from devices or microdrops to assess pre-implantation embryo metabolomics. As a control, spent media from devices without embryos was compared to media collected from microdrops without embryos using the same incubation time performed for embryo culture. These experiments were performed to investigate PDMS leaching and/or molecule absorption and adsorption. Spent culture media was frozen and stored at -80°C prior to sample preparation for analysis. Culture media samples (100μl) were thawed on ice and

prepared using previously described methods. Briefly, 300µl of dry ice cooled methanol was added to individual culture medium samples and incubated overnight at -80°C. Individual samples were spun down to remove proteins and the subsequent supernatant was used for analyses. Samples were separated and analysed using reverse-phase liquid chromatography connected to a Thermo Scientific Q Exactive HF (LC-Hybrid Quadrupole-Orbitrap MS/MS) instrument using positive ion mode MS [90–92]. MS raw data were imported, processed, normalized, and reviewed using Progenesis QI v.2.1 (Non-linear Dynamics, Newcastle, UK). Resulting MS data was utilized for relative quantitation. The full collection of raw data has been published on Metabolomics Workbench [93]. Tentative and putative annotations [94] were determined using accurate mass measurements (<5 ppm error), isotope distribution similarity, and manual assessment of fragmentation spectrum matching from the Human Metabolome Database (HMDB), [95] Metlin, [96] MassBank, [97] and the National Institute of Standards and Technology (NIST) database [98]. Increased confidence in the annotation of many features was achieved by manually assessing spectral match and RT consistencies between experimental data and chemical standards within a curated in-house library.

Statistical analysis

Data were analysed using GraphPad Prism 8 software (Graph Pad Software Inc., California, US). All data sets for first tested for fit to the normal distribution by D'Agostino-Pearson test for normality. In experiment 1, all normal data sets were compared by Student's t-test, while all non-parametric data were compared by Mann-Whitney U test. In experiment 2, all data sets were non-parametric and therefore tested for significant differences between groups by the Kruskal-Wallis test with post-hoc Dunn's test for multiple comparisons. In all instances, significance was determined as $P<0.05$. For metabolic activity experiments, results were checked for statistical differences between groups by ANOVA with post-hoc Bonferroni test. qPCR results were analysed by the comparative threshold cycle (C_t) method. Relative expression ratios were obtained using as internal control the mean of C_t values of 8 housekeeping genes from the sample of interest. Student t-test statistics was used to compare gene expression levels between samples from the different groups. Data was considered to be statistically different with a p value of <0.05. The values presented are means±sem for the numbers of samples/replicate cultures shown.

For MS, compounds with <20% coefficient of variance (%CV) were retained for further analysis. Within Progenesis QI, a one-way analysis of variance (ANOVA) test was used to assess significance between groups and returned a P-value for each feature (retention time_m/z descriptor), with a nominal P-value ≤ 0.05 required for significance. Significant features were further filtered using a fold change threshold ≥ |2| deemed as significant.

References

[1] N. B. Robinson *et al.*, "The current state of animal models in research: A review," *Int. J. Surg.*, vol. 72, pp. 9–13, Dec. 2019.

[2] A. L. Duran *et al.*, "Shared Ageing Research Models (ShARM): A new facility to support ageing research," *Biogerontology*, vol. 14, no. 6, pp. 789–794, Dec. 2013.

[3] R. Yuan, L. L. Peters, and B. Paigen, "Mice as a Mammalian Model for Research on the Genetics of Aging," *ILAR J.*, vol. 52, no. 1, pp. 4–15, Jan. 2011.

[4] R. Drost and J. Jonkers, "Opportunities and hurdles in the treatment of BRCA1-related breast cancer," *Oncogene*, vol. 33, no. 29. Nature Publishing Group, pp. 3753–3763, 17-Jul-2014.

[5] R. M. Drost and J. Jonkers, "Preclinical mouse models for BRCA1-associated breast cancer," *British Journal of Cancer*, vol. 101, no. 10. pp. 1651–1657, Nov-2009.

[6] J. Barr *et al.*, "Liquid Chromatography−Mass Spectrometry-Based Parallel Metabolic Profiling of Human and Mouse Model Serum Reveals Putative Biomarkers Associated

with the Progression of Nonalcoholic Fatty Liver Disease," *J. Proteome Res.*, vol. 9, no. 9, pp. 4501–4512, Sep. 2010.
[7] M. von Herrath and G. T. Nepom, "Remodeling rodent models to mimic human type 1 diabetes," *Eur. J. Immunol.*, vol. 39, no. 8, pp. 2049–2054, Aug. 2009.
[8] M. J. Prescott and K. Lidster, "Improving quality of science through better animal welfare: The NC3Rs strategy," *Lab Animal*, vol. 46, no. 4. Nature Publishing Group, pp. 152–156, Mar-2017.
[9] M. V. Wiles and R. A. Taft, "The sophisticated mouse: Protecting a precious reagent," *Methods Mol. Biol.*, vol. 602, pp. 23–36, 2010.
[10] S. P. Leibo and J. M. Sztein, "Cryopreservation of mammalian embryos: Derivation of a method," *Cryobiology*, vol. 86. Academic Press Inc., pp. 1–9, Feb-2019.
[11] K. H. Steele, J. M. Hester, B. J. Stone, K. M. Carrico, B. T. Spear, and A. Fath-Goodin, "Nonsurgical embryo transfer device compared with surgery for embryo transfer in mice," *J. Am. Assoc. Lab. Anim. Sci.*, vol. 52, no. 1, pp. 17–21, 2013.
[12] R. Bin Ali *et al.*, "Improved pregnancy and birth rates with routine application of nonsurgical embryo transfer," *Transgenic Res.*, vol. 23, no. 4, pp. 691–695, 2014.
[13] B. J. Stone, K. H. Steele, and A. Fath-Goodin, "A rapid and effective nonsurgical artificial insemination protocol using the NSET^{TM} device for sperm transfer in mice without anesthesia," *Transgenic Res.*, vol. 24, no. 4, pp. 775–781, Aug. 2015.
[14] R. L. Brinster, "A Method for in vitro cultivation of mouse ova from two-cell to blastocyst," *Exp. Cell Res.*, vol. 32, no. 1, pp. 205–208, 1963.
[15] M. A. Green, S. Bass, and B. T. Spear, "A device for the simple and rapid transcervical transfer of mouse embryos eliminates the need for surgery and potential post-operative complications," *Biotechniques*, vol. 47, no. 5, pp. 919–924, Nov. 2009.
[16] Abe Y., Nihon Sanka Fujinka Gakkai Zasshi. Factors influencing implantation of mouse embryos fertilized in vitro, 1988 Jul;40(7):821-7. Japanese. PMID: 3418190.
[17] Namiki, T, Ito, J, Kashiwazaki, N. Molecular mechanisms of embryonic implantation in mammals: Lessons from the gene manipulation of mice. *Reprod Med Biol*. 2018; 17: 331– 342.
[18] J. & T. Rossant P., "Mouse Development, Patterning, Morphogenesis, and Organogenesis.," *Acad. Press*, vol. 136, no. 1, pp. 371–389, 2002.
[19] C. S. Minot, *A laboratory text-book of embryology*. 2011.
[20] G. Kovacs, A. Rutherford, and D. K. Gardner, *How to Prepare the Egg and Embryo to Maximize IVF Success*. 2019.
[21] D. L. Hickman, D. J. Beebe, S. L. Rodriguez-Zas, and M. B. Wheeler, "Comparison of Static and Dynamic Medium Environments for Culturing of Pre-implantation Mouse Embryos," *Comp. Med.*, vol. 52, no. 2, pp. 122–126, 2002.
[22] L. Cabrera, Y. Heo, J. Ding, … S. T.-F. and, and U. 2006, "Improved blastocyst development with microfluidics and Braille pin actuator enabled dynamic culture," *Fertil. Steril.*, vol. 86, no. 3, p. S43, 2006.
[23] Y. Heo, L. Cabrera, and C. Bormann, "Dynamic microfunnel culture enhances mouse embryo development and pregnancy rates," *Hum. Reprod.*, vol. 25, no. 3, pp. 613–622, 2010.
[24] J. E. Swain, D. Lai, S. Takayama, and G. D. Smith, "Thinking big by thinking small: Application of microfluidic technology to improve ART," *Lab on a Chip*, vol. 13, no. 7. Royal Society of Chemistry, pp. 1213–1224, 07-Apr-2013.
[25] T. C. Esteves, F. Van Rossem, V. Nordhoff, S. Schlatt, M. Boiani, and S. Le Gac, "A microfluidic system supports single mouse embryo culture leading to full-term development," *RSC Adv.*, vol. 3, no. 48, pp. 26451–26458, Dec. 2013.
[26] P. L. Wale and D. K. Gardner, "The effects of chemical and physical factors on mammalian embryo culture and their importance for the practice of assisted human reproduction," *Hum. Reprod. Update*, vol. 22, no. 1, pp. 2–22, 2016.
[27] P. N. Zarmakoupis-Zavos and P. M. Zavos, "Factors that May Influence the Mouse Embryo Bioassay.," *Tohoku J. Exp. Med.*, vol. 179, no. 3, pp. 141–149, 1996.
[28] G. R. Holyoak, S. Wang, Y. Liu, and T. D. Bunch, "Toxic effects of ethylene oxide

residues on bovine embryos in vitro," *Toxicology*, vol. 108, no. 1–2, pp. 33–38, Apr. 1996.
[29] R. K. Naz, J. T. Janousek, T. Moody, and R. J. Stillman, "Factors influencing murine embryo bioassay: effects of proteins, aging of medium, and surgical glove coatings," 1986.
[30] M. Nijs, K. Franssen, A. Cox, D. Wissmann, H. Ruis, and W. Ombelet, "Reprotoxicity of intrauterine insemination and in vitro fertilization-embryo transfer disposables and products: a 4-year survey," *Fertil. Steril.*, vol. 92, no. 2, pp. 527–535, Aug. 2009.
[31] A. E. Ongaro *et al.*, "Polylactic acid, a sustainable, biocompatible, transparent substrate material for Organ-On-Chip, and Microfluidic applications," *bioRxiv*, p. 647347, 2019.
[32] S. Raty *et al.*, "Embryonic development in the mouse is enhanced via microchannel culture.," *Lab Chip*, vol. 4, pp. 186–190, 2004.
[33] D. E. Morbeck, "Mouse embryo assay for quality control in the IVF laboratory," in *Principles of IVF Laboratory Practice: Optimizing Performance and Outcomes*, Cambridge University Press, 2017, pp. 69–72.
[34] J. A. B. M. Abdullah, "Continuous ultra micro-drop (cUMD) culture yields higher pregnancy and implantation rates than either larger-drop culture or fresh-medium replacement." 2004.
[35] R. S. Canseco, A. E. T. Sparks, R. E. Pearson, and F. C. Gwazdauskas, "Embryo density and medium volume effects on early murine embryo development," *J. Assist. Reprod. Genet.*, vol. 9, no. 5, pp. 454–457, Oct. 1992.
[36] B. C. Paria and S. K. Dey, "Preimplantation embryo development in vitro: Cooperative interactions among embryos and role of growth factors," *Proc. Natl. Acad. Sci. U. S. A.*, vol. 87, no. 12, pp. 4756–4760, 1990.
[37] M. Lane and D. K. Gardner, "Effect of incubation volume and embryo density on the development and viability of mouse embryos in vitro," *Hum. Reprod.*, vol. 7, no. 4, pp. 558–562, Apr. 1992.
[38] Assessment of Mammalian Embryo Quality - Invasive and non-invasive techniques, 2002 Editors: van Soom, A., Boerjan, M., Kluwer Academic Publishers, 2002.
[39] B. Balaban and B. Urman, "Effect of oocyte morphology on embryo development and implantation," *Reprod. Biomed. Online*, vol. 12, no. 5, pp. 608–615, 2006.
[40] T. Ebner, "Selection based on morphological assessment of oocytes and embryos at different stages of preimplantation development: a review," *Hum. Reprod. Update*, vol. 9, no. 3, pp. 251–262, May 2003.
[41] Y. Yu *et al.*, "Assessment of the developmental competence of human somatic cell nuclear transfer embryos by oocyte morphology classification," *Hum. Reprod.*, vol. 24, no. 3, pp. 649–657, Dec. 2008.
[42] G. Coticchio, E. Sereni, L. Serrao, and et al., "What Criteria for the Definition of Oocyte Quality?," *Ann. N. Y. Acad. Sci.*, vol. 1034, no. 1, pp. 132–144, Dec. 2004.
[43] R. L. Krisher, "The effect of oocyte quality on development.," *Journal of animal science*, vol. 82 E-Suppl. 2004.
[44] F. Guerif, P. J. Mckeegan, H. J. Leese, and R. G. Sturmey, "A simple approach for COnsumption and RElease (CORE) analysis of metabolic activity in single mammalian embryos.," *PLoS One*, vol. 8, no. 8, p. e67834, Jan. 2013.
[45] H. J. Leese, F. Guerif, V. Allgar, D. R. Brison, K. Lundin, and R. G. Sturmey, "Biological optimization, the Goldilocks principle, and how much is lagom in the preimplantation embryo," *Mol. Reprod. Dev.*, Jul. 2016.
[46] P. J. McKeegan and R. G. Sturmey, "Metabolomic Screening of Embryos to Enhance Successful Selection and Transfer," in *How to Prepare the Egg and Embryo to Maximize IVF Success*, A. Rutherford, D. K. Gardner, and G. Kovacs, Eds. Cambridge: Cambridge University Press, 2019, pp. 295–304.
[47] J. F. Schultz and D. R. Armant, "β1- and β3-class integrins mediate fibronectin binding activity at the surface of developing mouse peri-implantation blastocysts: Regulation by ligand-induced mobilization of stored receptor," *J. Biol. Chem.*, vol. 270, no. 19, pp. 11522–11531, May 1995.

[48] G. A. Thouas, A. O. Trounson, E. J. Wolvetang, and G. M. Jones, “Mitochondrial dysfunction in mouse oocytes results in preimplantation embryo arrest in vitro.,” *Biol. Reprod.*, vol. 71, no. 6, pp. 1936–42, Dec. 2004.
[49] G. Leppens, D. K. Gardner, and D. Sakkas, “Co-culture of 1-cell outbred mouse embryos on bovine kidney epithelial cells: effect on development, glycolytic activity, inner cell mass: trophectoderm ratios and viability,” *Hum. Reprod.*, vol. 11, no. 3, pp. 598–600, Mar. 1996.
[50] N. K. Binder, N. J. Hannan, and D. K. Gardner, “Paternal diet-induced obesity retards early mouse embryo development, mitochondrial activity and pregnancy health.,” *PLoS One*, vol. 7, no. 12, p. e52304, Jan. 2012.
[51] T. Hamatani, M. G. Carter, A. A. Sharov, and M. S. H. Ko, “Dynamics of global gene expression changes during mouse preimplantation development,” *Dev. Cell*, vol. 6, no. 1, pp. 117–131, Jan. 2004.
[52] Q. T. Wang *et al.*, “A genome-wide study of gene activity reveals developmental signaling pathways in the preimplantation mouse embryo,” *Dev. Cell*, vol. 6, no. 1, pp. 133–144, Jan. 2004.
[53] J. Adjaye *et al.*, “Primary Differentiation in the Human Blastocyst: Comparative Molecular Portraits of Inner Cell Mass and Trophectoderm Cells,” *Stem Cells*, vol. 23, no. 10, pp. 1514–1525, 2005.
[54] R. Yagi *et al.*, “Transcription factor TEAD4 specifies the trophectoderm lineage at the beginning of mammalian development.,” *Development*, vol. 134, no. 21, pp. 3827–36, Nov. 2007.
[55] R. K. Ng *et al.*, “Epigenetic restriction of embryonic cell lineage fate by methylation of Elf5,” vol. 10, no. 11, 2008.
[56] A. Suwińska, R. Czołowska, W. Ozdzeński, and A. K. Tarkowski, “Blastomeres of the mouse embryo lose totipotency after the fifth cleavage division: Expression of Cdx2 and Oct4 and developmental potential of inner and outer blastomeres of 16- and 32-cell embryos,” *Dev. Biol.*, vol. 322, no. 1, pp. 133–144, Oct. 2008.
[57] B. Hendrich, J. Guy, B. Ramsahoye, V. A. Wilson, and A. Bird, “Closely related proteins MBD2 and MBD3 play distinctive but interacting roles in mouse development,” *Genes Dev.*, vol. 15, no. 6, pp. 710–723, Mar. 2001.
[58] J. Kim, S. H. Kim, and J. H. Jun, “Prediction of blastocyst development and implantation potential in utero based on the third cleavage and compaction times in mouse pre-implantation embryos,” *J. Reprod. Dev.*, vol. 63, no. 2, pp. 117–125, 2017.
[59] L. Chen, D. Wang, Z. Wu, L. Ma, and G. Q. Daley, “Molecular basis of the first cell fate determination in mouse embryogenesis,” *Cell Research*, vol. 20, no. 9. pp. 982–993, Sep-2010.
[60] A. Manbachi *et al.*, “Microcirculation within grooved substrates regulates cell positioning and cell docking inside microfluidic channels,” *Lab Chip*, vol. 8, no. 5, p. 747, Apr. 2008.
[61] J.-B. Bao and D. Jed Harrison, “Measurement of flow in microfluidic networks with micrometer-sized flow restrictors,” *AIChE J.*, vol. 52, no. 1, pp. 75–85, Jan. 2006.
[62] J.F. Schultz, L. Mayernik, U.K. Rout, D.R. Armant, "Integrin trafficking regulates adhesion to fibronectin during differentiation of mouse peri-implantation blastocysts," *Dev. Genet.* 21, 31–43, 1997.
[63] Y. Kaneko, C.R. Murphy, M.L. Day, "Extracellular matrix proteins secreted from both the endometrium and the embryo are required for attachment: a study using a co-culture model of rat blastocysts and Ishikawa cells," *J. Morphol.* 274, 63–72, 2013.
[64] J. Van Blerkom, “Domains of high-polarized and low-polarized mitochondria may occur in mouse and human oocytes and early embryos,” *Hum. Reprod.*, 17, 2, 393–406, Feb. 2002.
[65] H. Ge et al., “The importance of mitochondrial metabolic activity and mitochondrial DNA replication during oocyte maturation in vitro on oocyte quality and subsequent embryo developmental competence,” *Mol. Reprod. Dev.,* 79, 6, 392–401, Jun. 2012.
[66] F.D. Houghton, J. G. Thompson, C. J. Kennedy, and H. J. Leese, “Oxygen consumption and energy metabolism of the early mouse embryo,” *Mol. Reprod. Dev.*, vol. 44, no. 4,

pp. 476–85, Aug. 1996.
[67] Kay, Graham F., et al. "Expression of Xist during mouse development suggests a role in the initiation of X chromosome inactivation." Cell 72.2 (1993): 171-182
[68] Y. Watanabe *et al.*, “Notch and Hippo signaling converge on Strawberry Notch 1 (Sbno1) to synergistically activate Cdx2 during specification of the trophectoderm,” *Sci. Rep.*, vol. 7, no. 1, p. 46135, May 2017.
[69] S. C. J. Lin, M. A. Wani, J. A. Whitsett, and J. M. Wells, “Klf5 regulates lineage formation in the pre-implantation mouse embryo,” *Development*, vol. 137, no. 23, pp. 3953–3963, 2010.
[70] P. Home, S. Ray, D. Dutta, I. Bronshteyn, M. Larson, and S. Paul, “GATA3 Is Selectively Expressed in the Trophectoderm of Peri-implantation Embryo and Directly Regulates Cdx2 Gene Expression,” *J. Biol. Chem.*, vol. 284, no. 42, p. 28729, 2009.
[71] M. Ozawa *et al.*, “Global gene expression of the inner cell mass and trophectoderm of the bovine blastocyst,” *BMC Dev. Biol.*, vol. 12, no. 1, p. 33, Nov. 2012.
[72] X.-S. Cui, X.-H. Shen, and N.-H. Kim, “Dicer1 expression in preimplantation mouse embryos: Involvement of Oct3/4 transcription at the blastocyst stage,” *Biochem. Biophys. Res. Commun.*, vol. 352, no. 1, pp. 231–236, Jan. 2007.
[73] C. Chazaud and Y. Yamanaka, “Lineage specification in the mouse preimplantation embryo.,” *Development*, vol. 143, no. 7, pp. 1063–74, Apr. 2016.
[74] M. A. Avila, E. R. García-Trevijano, S. C. Lu, F. J. Corrales, and J. M. Mato, “Methylthioadenosine,” *International Journal of Biochemistry and Cell Biology*, vol. 36, no. 11. Elsevier Ltd, pp. 2125–2130, 01-Nov-2004.
[75] M. Alexiou and H. J. Leese, “Purine utilisation, de novo synthesis and degradation in mouse preimplantation embryos,” *Development*, 114, 1, 1992.
[76] Sajal Gupta, J. Banerjee, and A. Agarwal, “The Impact of Reactive Oxygen Species on Early Human Embryos: A Systematic Review of the Literature,” 2006.
[77] Kim J, Lee J, Jun JH. Advantages of the outgrowth model for evaluating the implantation competence of blastocysts. *Clin Exp Reprod Med*, vol. 47, no. 2, p.85-93, 2020.
[78] K. J. Regehr *et al.*, “Biological implications of polydimethylsiloxane-based microfluidic cell culture,” *Lab Chip*, vol. 9, no. 15, p. 2132, 2009.
[79] E. Berthier, E. W. K. Young, and D. Beebe, “Engineers are from PDMS-land, Biologists are from Polystyrenia,” *Lab Chip*, 12, 7, 1224, Mar. 2012.
[80] J. Ali, W.K. Whitten, J.N. Shelton, "Effect of culture systems on mouse early embryo development", *Human Reprod.,* 8, 7, 1110–1114, July 1993.
[81] S. G. Charati and S. A. Stern, "Diffusion of Gases in Silicone Polymers: Molecular Dynamics Simulations Macromolecules," *Macromolecules,* 31, 16, 5529-5535, 1998.
[82] S. Hitoshi, S. Takeshi, W. Ching-Chou, Y. Tomoyuki, Y. Masaki, A. Hiroyuki, M. Tomokazu, Y. Hiroshi, "Oxygen Permeability of Surface-modified Poly(dimethylsiloxane) Characterized by Scanning Electrochemical Microscopy," *Chemistry Letters*, 35, 2, 234-235, 2006.
[83] B. Fischer and B. D. Bavister, “Oxygen tension in the oviduct and uterus of rhesus monkeys, hamsters and rabbits.,” *J. Reprod. Fertil.*, vol. 99, no. 2, pp. 673–9, Nov. 1993.
[84] N. M. Orsi and H. J. Leese, “Protection against reactive oxygen species during mouse preimplantation embryo development: role of EDTA, oxygen tension, catalase, superoxide dismutase and pyruvate.,” *Mol. Reprod. Dev.*, vol. 59, no. 1, pp. 44–53, May 2001.
[85] M. Meintjes *et al.*, “A controlled randomized trial evaluating the effect of lowered incubator oxygen tension on live births in a predominantly blastocyst transfer program.,” *Hum. Reprod.*, vol. 24, no. 2, pp. 300–7, Feb. 2009.
[86] CRACK IT Review 2019, pp.40-43, https://www.nc3rs.org.uk/sites/default/files/documents/Corporate_publications/Research_Reviews/CRACK%20IT%20Review%202019.pdf.
[87] N. J. Hannan, P. Paiva, K. L. Meehan, L. J. F. Rombauts, D. K. Gardner, and L. A. Salamonsen, “Analysis of Fertility-Related Soluble Mediators in Human Uterine Fluid

Identifies VEGF as a Key Regulator of Embryo Implantation," *Endocrinology*, 152, 12, 4948–4956, Dec. 2011.
[88] S. Picelli, O. R. Faridani, Å. K. Björklund, G. Winberg, S. Sagasser, and R. Sandberg, "Full-length RNA-seq from single cells using Smart-seq2," *Nat. Protoc.*, vol. 9, no. 1, pp. 171–181, 2014.
[89] K. J. Regehr *et al.*, "Biological implications of polydimethylsiloxane-based microfluidic cell culture," *Lab Chip*, vol. 9, no. 15, p. 2132, 2009.
[90] S. A. Chambers *et al.*, "A solution to antifolate resistance in group B streptococcus: Untargeted metabolomics identifies human milk oligosaccharide-induced perturbations that result in potentiation of trimethoprim," *MBio*, vol. 11, no. 2, Mar. 2020.
[91] A. R. Eberly *et al.*, "Defining a Molecular Signature for Uropathogenic versus Urocolonizing Escherichia coli: The Status of the Field and New Clinical Opportunities," *J. Mol. Biol.*, vol. 432, no. 4, pp. 786–804, Feb. 2020.
[92] J. A. Brown *et al.*, "Metabolic consequences of interleukin-6 challenge in developing neurons and astroglia," *J. Neuroinflammation*, vol. 11, no. 1, p. 183, Nov. 2014.
[93] Metabolomics Workbench: An international repository for metabolomics data and metadata, metabolite standards, protocols, tutorials and training, and analysis tools. Sud M et al. 2016, *Nucleic Acids Research*, 44(D1):D463-70 Project https://doi.org/10.21228/M8W99G.
[94] A. C. Schrimpe-Rutledge, S. G. Codreanu, S. D. Sherrod, and J. A. McLean, "Untargeted Metabolomics Strategies—Challenges and Emerging Directions," *J. Am. Soc. Mass Spectrom.*, vol. 27, no. 12, pp. 1897–1905, Dec. 2016.
[95] D. Wishart, T. Jewison, A. Guo, … M. W.-N. acids, and undefined 2012, "HMDB 3.0—the human metabolome database in 2013," *academic.oup.com*.
[96] "METLIN: a metabolite mass spectral database," *journals.lww.com*.
[97] H. Horai *et al.*, "MassBank: a public repository for sharing mass spectral data for life sciences," *J. Mass Spectrom.*, vol. 45, no. 7, pp. 703–714, Jul. 2010.
[98] A. Jablonski, "NIST Standard Reference Database 64 NIST Electron Elastic-Scattering Cross-Section Database," 2010.

Acknowledgments
We would like to thank Mr. F. Colucci for lab work and design contribution in the first experimental phase of the project, and Miss C. Espinilla Aguilar that contributed to the loading capacity experiment and analysis of polarisation ratio.
This project has been sponsored by the Medical Research Council Harwell Institute through the NC3Rs CRACK IT EASE Challenge (CRACKITEA-SP-3). It has been partially funded by the MRC CiC5- Confidence in Concept 2018/19 (MC_PC_17165). This project has received funding from the European Union's Horizon 2020 research and innovation programme under the Marie Skłodowska-Curie grant agreement No 748903.

Author Contribution
V. Mancini participated in the design and optimization of the embryo culture device, design and completion of the qPCR analysis and the generation and analysis of samples for MS analysis. Vanessa is now in a new position at the Department of Anatomy & Embryology, Leiden University Medical Center, Einthovenweg 20, 2333 ZC, Leiden, The Netherlands.
P. McKeegan carried out the experimental validation of the device, organized the embryo culture work and completed the analysis of cleavage and blastocyst rates blastocyst cell number and outgrowth, mitochondrial polarisation ratios and energy metabolism measurements.
A.C. Rutledge performed metabolomics data processing and management of annotation activities; provided supervision and applied statistical techniques to study data. She also critically reviewed, and provided commentary and revision to the manuscript.
S.G. Codreanu designed the LC-MS/MS analytical method; processed the samples for metabolomics analysis and collected the MS data. She verified the overall quality and

reproducibility of the results; provided revisions to the final manuscript.
S.D. Sherrod defined the best analytical method for the untargeted metabolomics analysis using the effluent from the microfluidic system. She mentored the core team on the metabolomics research activity, planning and execution as well as critically reviewed, and provided commentary and revision to the final manuscript.
J.A. McLean provided all the resources available for the metabolomic studies, including: reagents, materials, instrumentation, and computational resources for the metabolomics analysis. He also provided commentary and revision to the final manuscript.
H.M Picton defined the specifics for design and use of the microfluidic systems and provided guideline for the definition of a clinically relevant device. She led on the strategy used for all embryo culture experiments, embryo quality assessments and culture endpoints. She major editorial input on the manuscript and advised on the expectations and needs in the field.
V. Pensabene conceived the device design and characteristics and promoted its use in animal and human IVF. She defined the experimental protocols used for validation of device design and analytical methods and defined the full manuscript structure, provided guidance to the co-authors for the different activities and wrote introduction and conclusions.

Additional Information

Supplementary information
Video 1 Loading
Video 2 Retrieval

Competing interest

The Authors do not have any conflict of interest with the described research results.

Figures

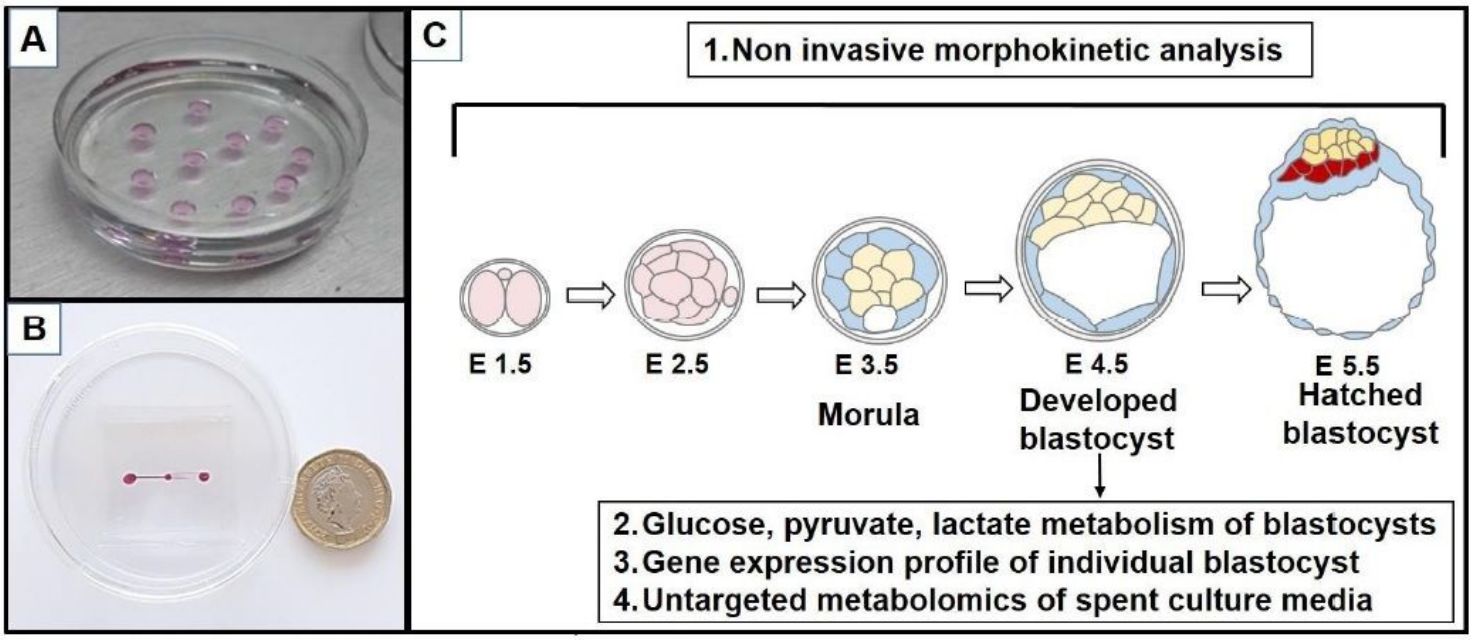

Figure 1

A) Traditional microdrop culture. B) Image of the fabricated PDMS microfluidic device in a traditional 60 mm petri dish used for embryo culture. Red dye indicates inlet and outlet ports and microfluidic channels. The device is sitting within a standard 60mm culture dish. Image shown next to a UK 1 pound coin for scale. C) Schematic of in vitro murine embryo development in the device. Non-invasive analytical methods can be used to monitor, grade and stage the embryos during culture. Endpoint embryo quality analyses (genetic and metabolic profiling) that can be performed for each individual embryo.

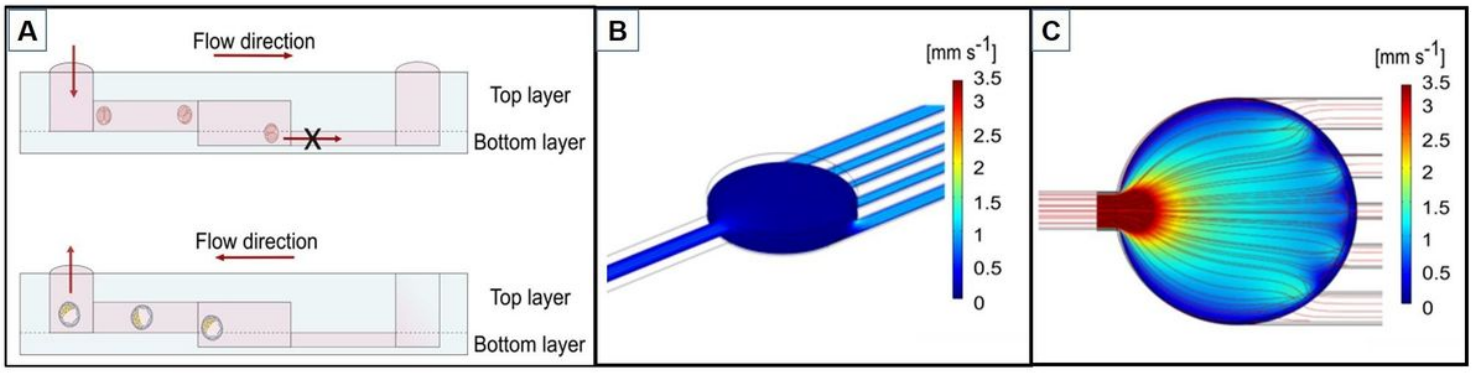

Figure 2

Microfluidic device design. A) Embryos are introduced from the inlet port, guided by capillarity force in the culture chamber through the inlet channel. Being the embryos diameter bigger than the outlet channels, they remain trapped in the chamber. Once developed embryos are aspirated from the inlet port. B) The Finite Element Model of the average velocity shows an increase in the lateral channels compared to the

main chamber owing to their small dimensions. C) Fluid flow analysis of velocity magnitude surface plot shows the velocity field generated in the fluidic systems.

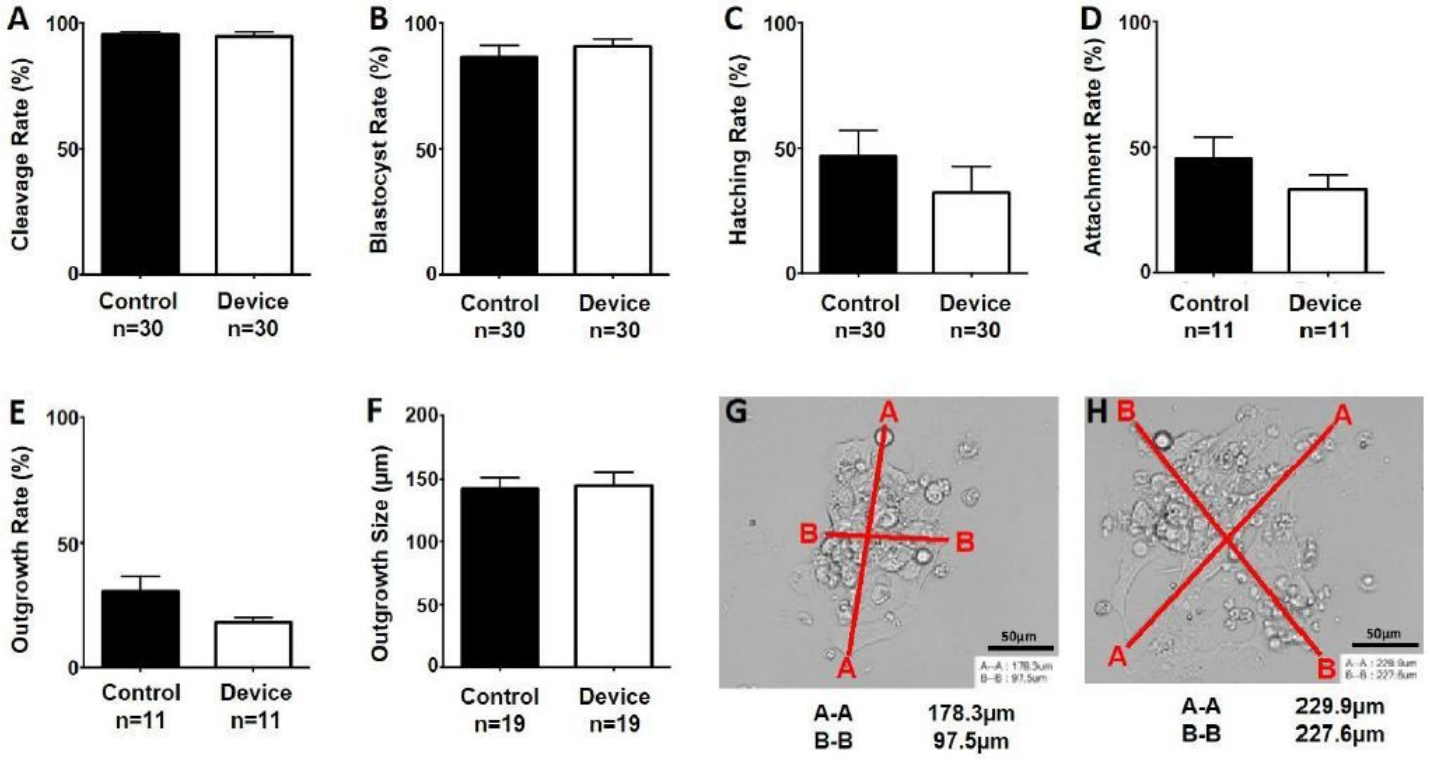

Figure 3

Comparison of preimplantation embryo development. A) Cleavage rates (94.62 ± 1.7%, n=30 vs control 94.84 ± 1.08%, n=30, p=0.48). B) Blastocyst rates (out of total embryos cultured) (90.48 ± 3.2%, n=30 vs control 86.40 ± 4.6%, n=30, p=0.6), C) Hatching rates (out of total blastocysts) (32.18 ± 10.35%, n=30 vs control 46.61 ± 10.28%, n=30, p=0.32), D) Attachment rates (out of total blastocysts) (33.22 ± 5.6%, n=11 vs control 45.64 ± 8.4%, n=11, p=0.35), E) Outgrowth rates (out of total blastocysts) (18.2 ± 1.9%, n=11 vs control 30.6 ± 6.0%, n=11, p=0.08), F) Mean outgrowth size (µm) (144.5 ± 11.0 µm, n=19 vs control 142.1 ± 9.0 µm, n=19, p=0.72). Values plotted are means±sem for the number of embryos. G-H) Representative images of blastocyst outgrowth by embryos cultured in microdrops and microfluidic devices respectively: red lines indicate measurement bars created in RI viewer (A-A and B-B). Scale bar 50 µm.

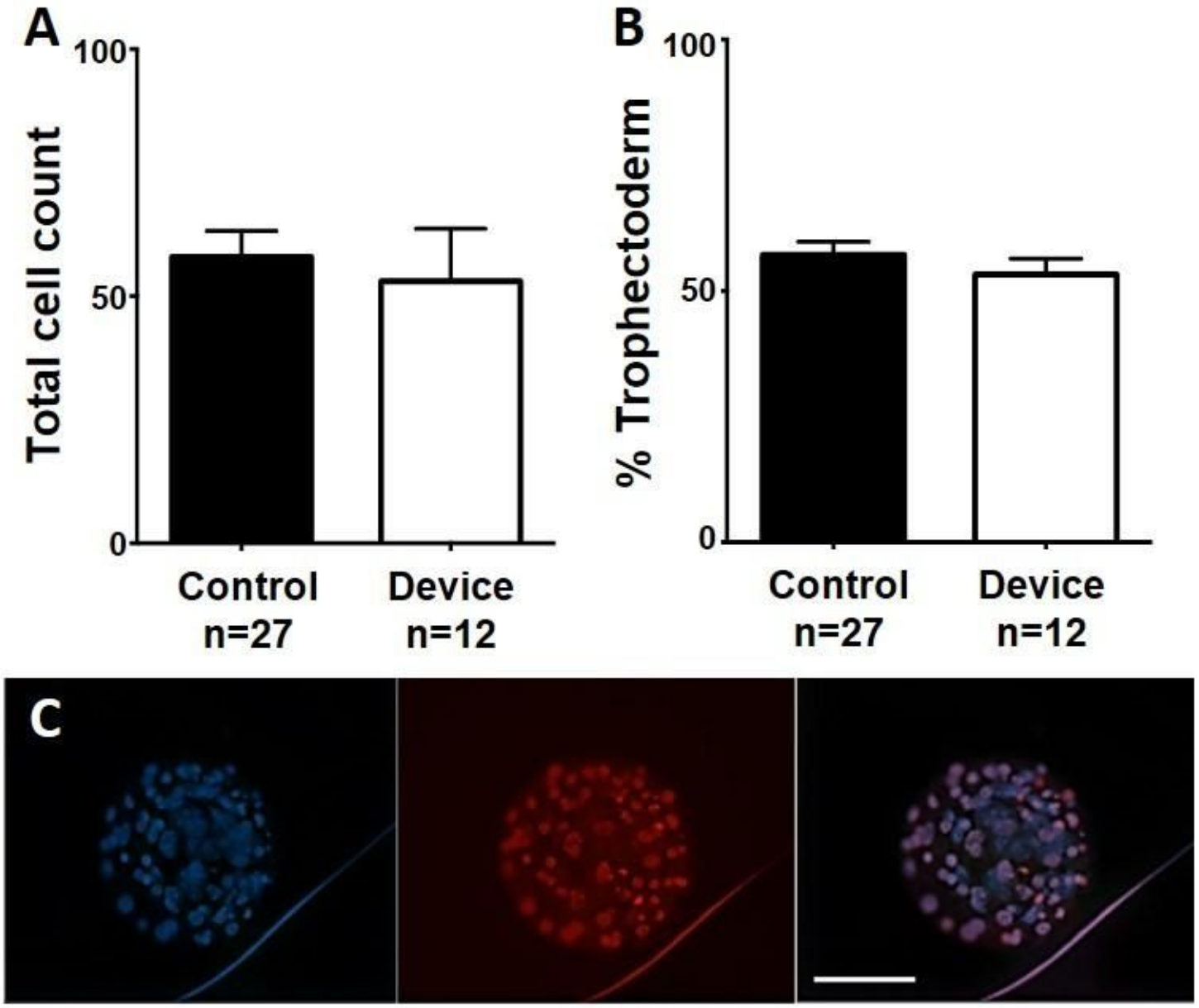

Figure 4

A) Total cell count 53±10.6 cells, n=12 embryos, p=0.6 vs control 58± 5.2 cells, n=27 embryos. B) Cell allocation ratio (% Trophectoderm) 53.3±3.2%TE, n=12, p=0.4 vs control 57.2±2.6%TE, n=27, p=0.4. Values plotted are means±sem for the number of embryos analysed. C) Representative conventional epifluorescent image of blastocyst within the device stained with Hoechst 3342 and Propidium Iodide and imaged in the 460nm (blue) and 560nm (red) channels respectively. Scale bar 50 μm.

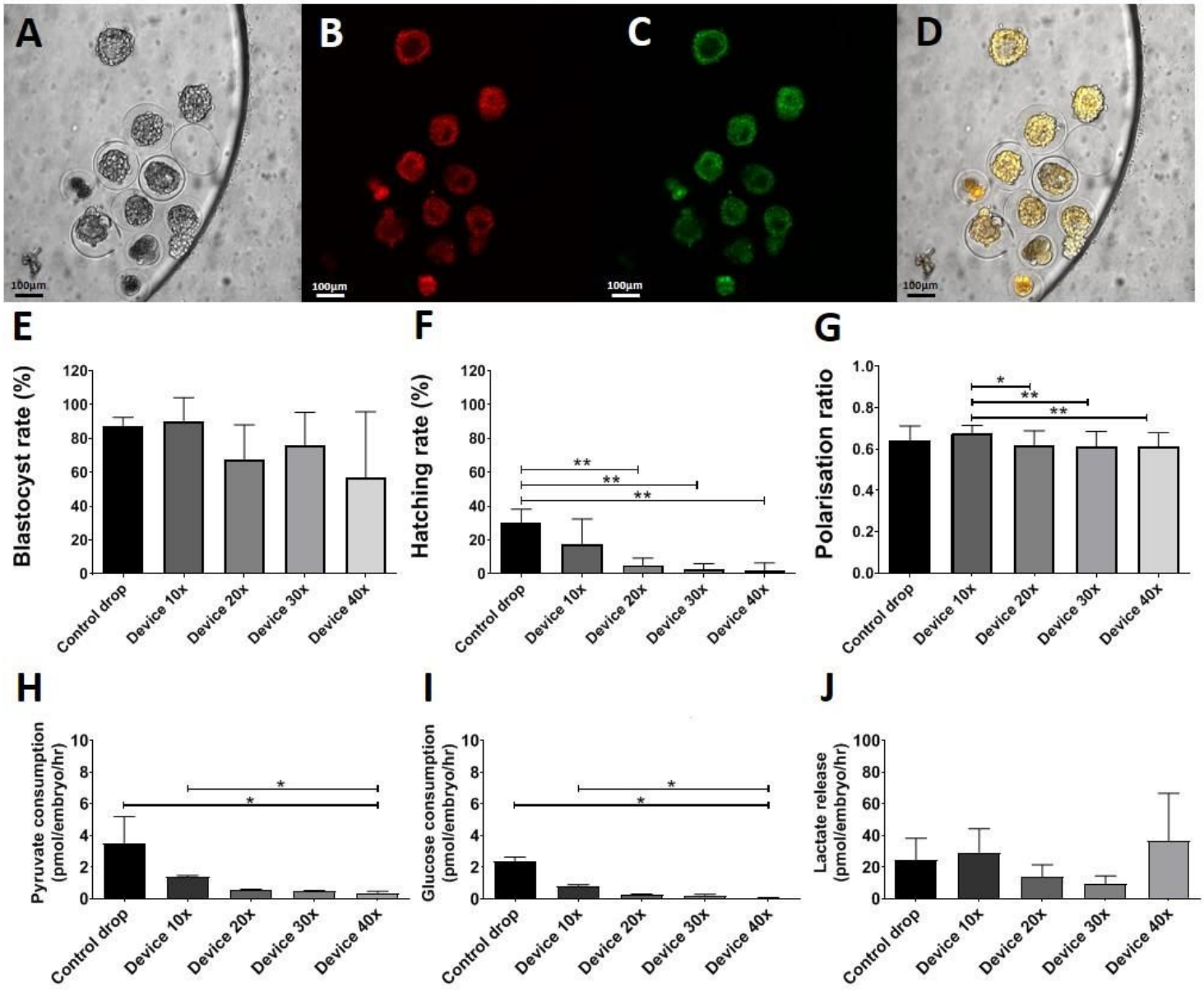

Figure 5

Loading capacity experiment. A) Brightfield, B-D) Analysis of mitochondrial polarisation ratio. Representative conventional epifluorescent images of blastocysts within the device stained with the potentiometric mitochondria-specific stain JC-10 and imaged in the rhodamine isothiocyanate (RITC, B) and fluorescein isothiocyanate (FITC, C) channels respectively. Scale bar 100 µm. E) Blastocyst rate (n=4) F) Hatching rate (n=4) G). Quantified blastocyst polarisation ratio data (n=4) shows higher value when culturing groups of 10 embryos inside the device. H-J) Energy substrate turnover (n=4).the 5 replicate cultures. *indicates significant differences at P<0.05.

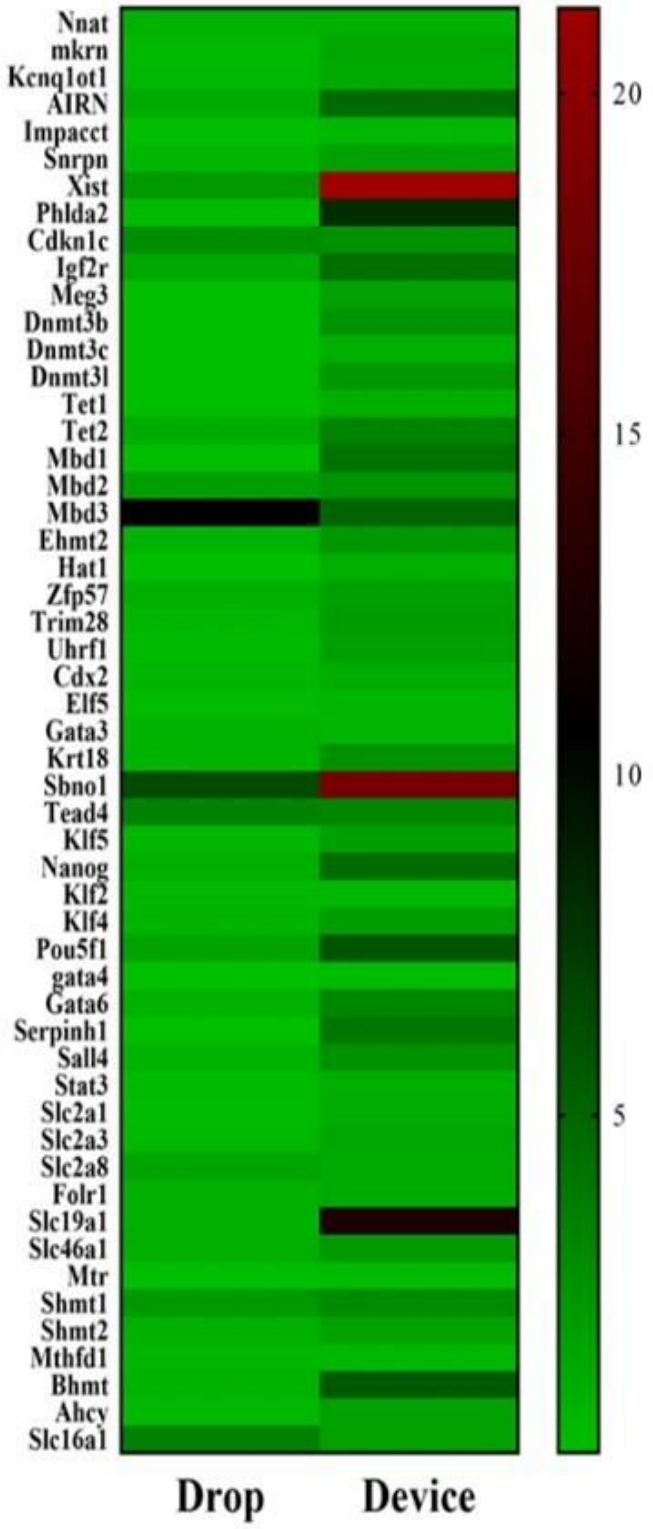

Figure 6

Heatmap representing gene expression of mouse blastocysts cultured in the device compared to microdrop culture. Scale: red indicates high expression and green is low expression.

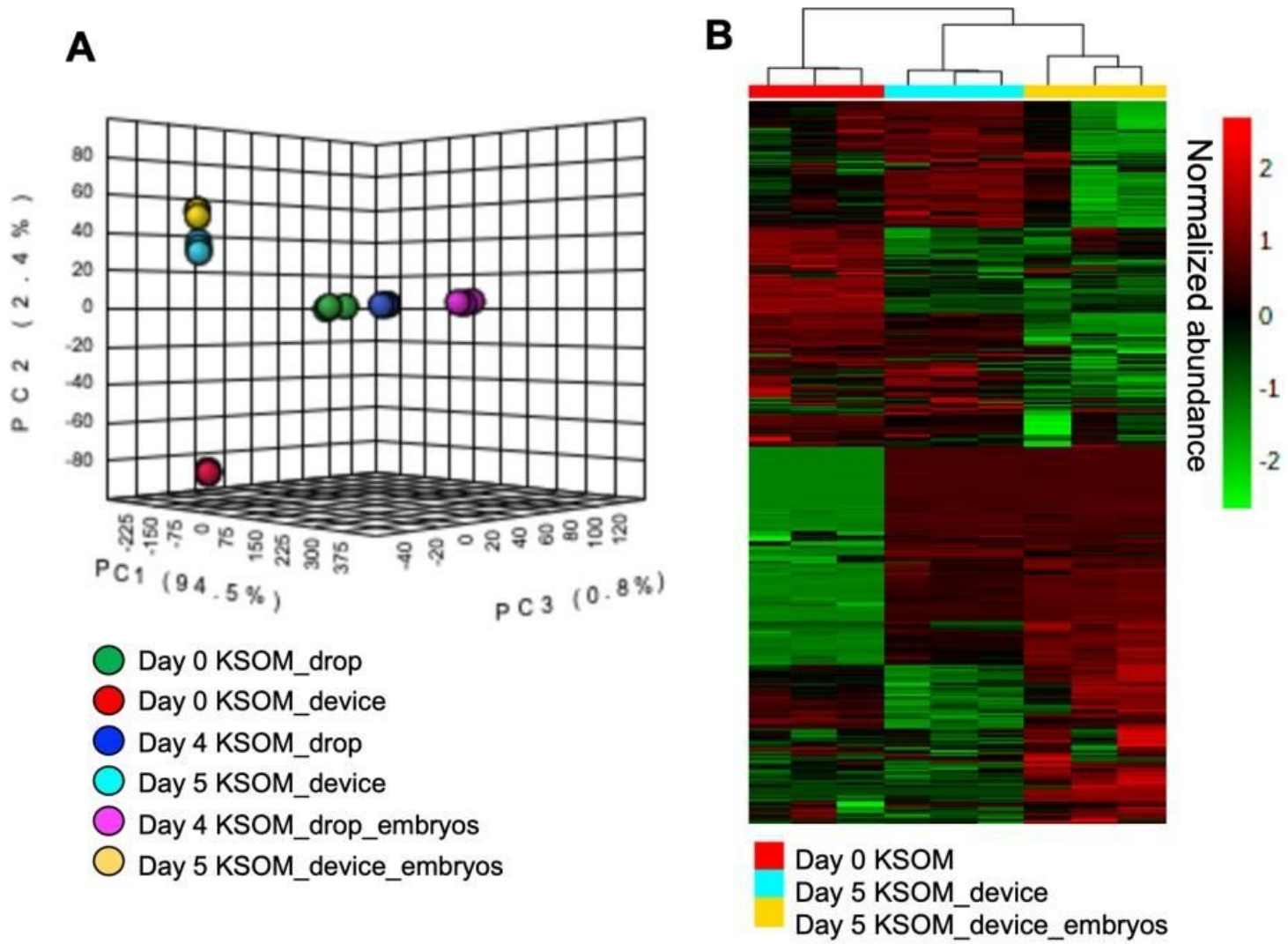

Figure 7

Principal Component Analysis (PCA) and heatmap visualization of global, untargeted mass spectrometry. (A) PCA plot of the LC-MS/MS data of medium samples from devices after 4 days in microdrops or 5 days in devices and control KSOM (n=3 replicate cultures per experimental group). (B) Heatmap analysis of media samples collected from the microfluidic device with and without embryos. Sample replicates are visualized in columns column based on hierarchical clustering, with metabolites presented on individual rows. Species are colored based on normalized abundance from red (high) to green (low).

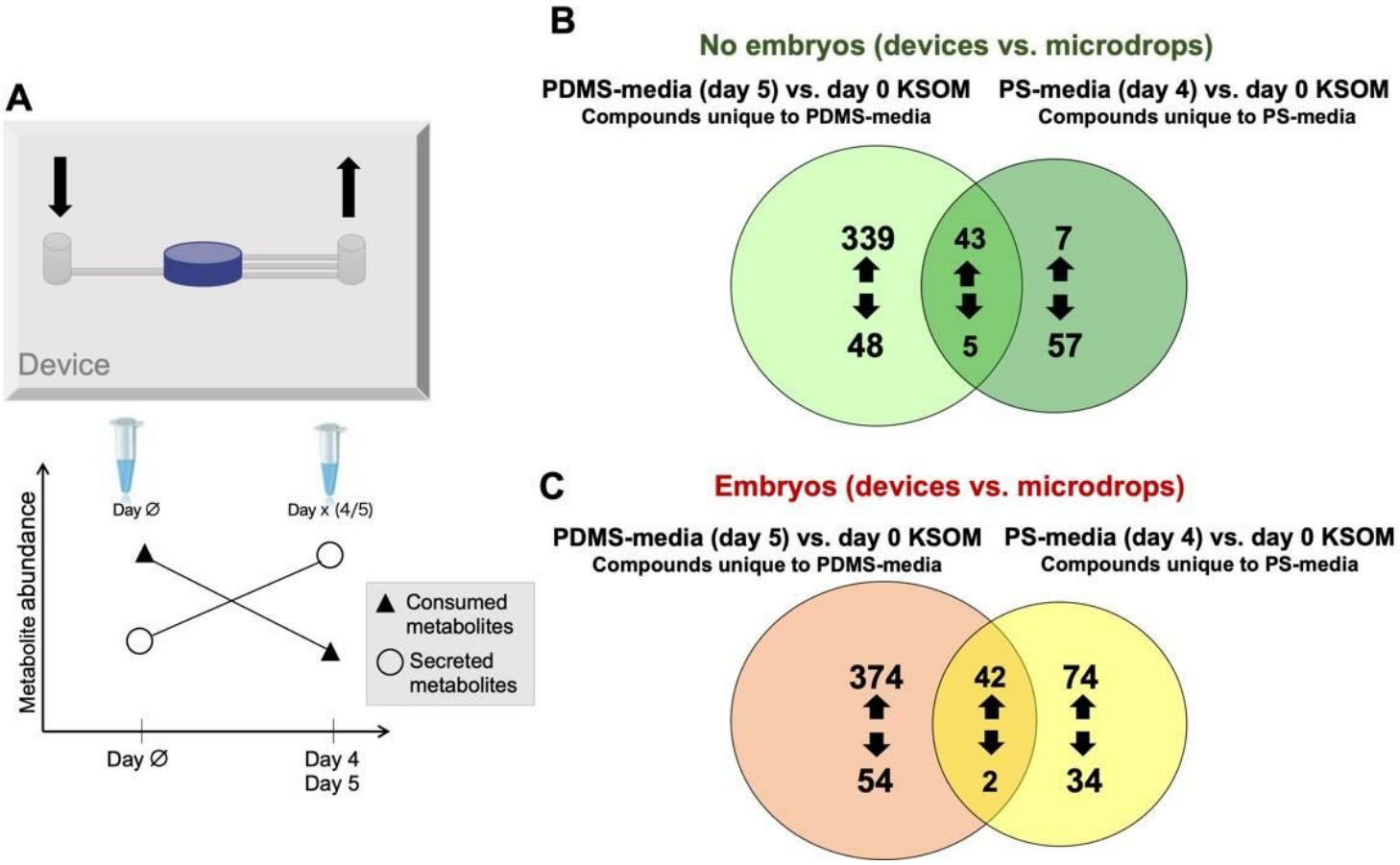

Figure 8

Venn diagram of dysregulated compounds in PDMS-media and PS-media compared to control (day 0 KSOM). (A) Schematic of the device with arrows indicating inlet (⇩) and outlet (⇧) ports (top). Changes in metabolite abundance in samples collected from microdrops (day 4) or devices (day 5) when compared to control. Increased and decreased compounds represent, respectively, released and consumed metabolites (bottom). (B) Comparison of dysregulated compounds in day 5 PDMS-media and day 4 PS-media without embryos. (C) Comparison of dysregulated compounds in day 5 embryo culture PDMS-media and day 4 embryo culture PS-media.

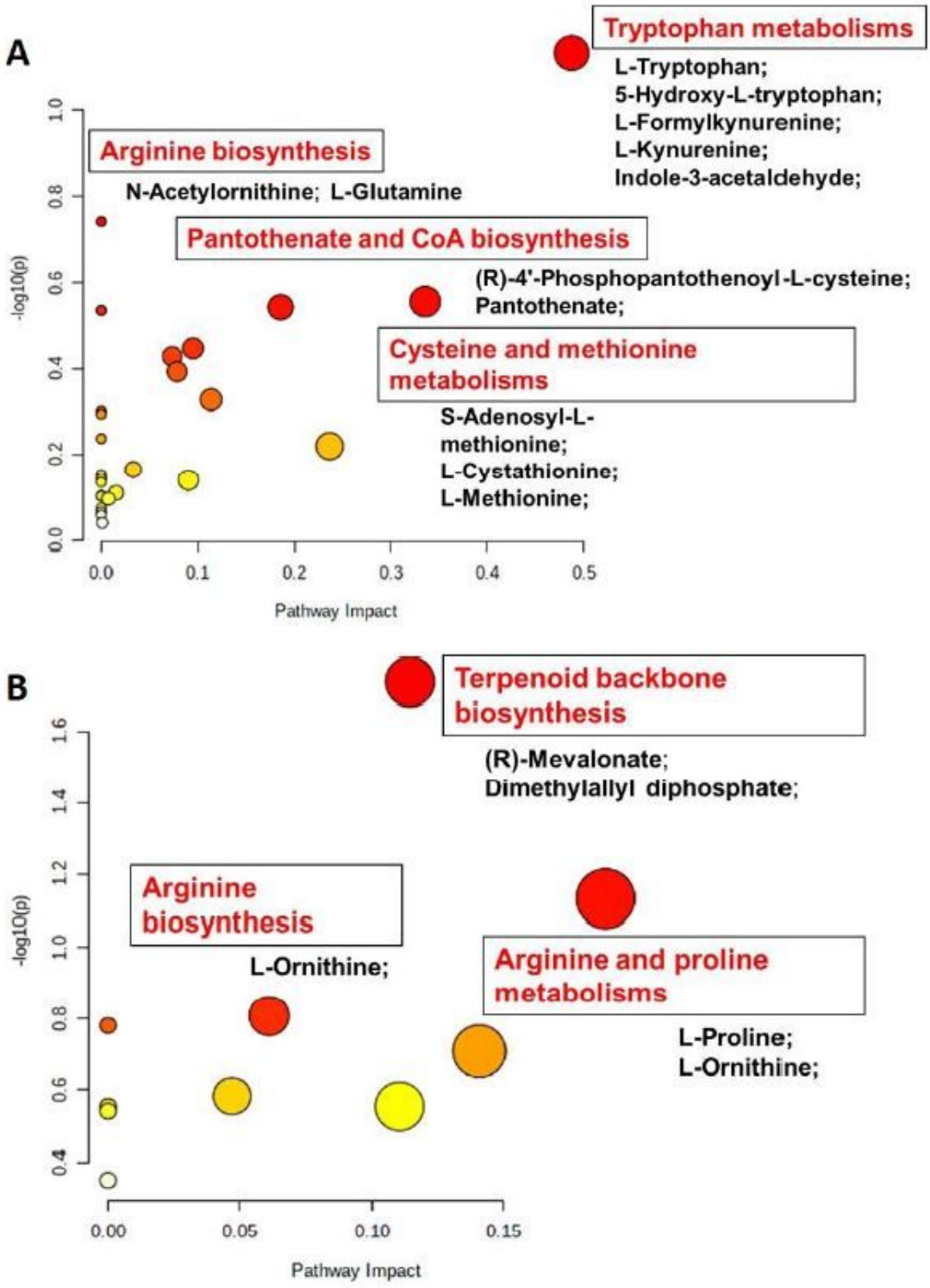

Figure 9

Pathways overrepresentation analysis. Summary of metabolic pathways of significant metabolites uniquely up-regulated in day 5 embryo culture PDMS-media (vs. day 0 KSOM) (A) and in day 4 embryo culture PS-media (vs. day 0 KSOM) (B). The metabolome view contains results of the analysis generated by Metaboanalyst with all the matched pathways arranged by p-values on Y-axis, and pathway impact values on X-axis.

Supplementary Files

This is a list of supplementary files associated with this preprint. Click to download.

- Supplementarymaterial05022021.pdf
- Supplementaryvideos.pptx